Bis(Amino Acid) Oxalyl Amides as Ambidextrous Gelators of Water and Organic Solvents: Supramolecular Gels with Temperature Dependent Assembly/Dissolution Equilibrium

Janja Makarević,[a] Milan Jokić,[a] Berislav Perić,[b] Vladislav Tomišić,[c] Biserka Kojić-Prodić,*[b] and Mladen Žinić*[a]

Abstract: Bis(LeuOH) (**1a**), bis(ValOH) (**2a**) and bis(PhgOH) (**5a**) (Phg denotes (*R*)-phenylglycine) oxalyl amides are efficient low molecular weight organic gelators of various organic solvents and their mixtures as well as water, water/DMSO, and water/DMF mixtures. The organisational motifs in aqueous gels are dominated primarily by lipophilic interactions while those in organic solvents are formed by intermolecular hydrogen bonding. Most of the gels are thermoreversible and stable for many months. However, **2a** forms unstable gels with organic solvents which upon ageing transform into variety of crystalline shapes. For some **1a**/alcohol gels, a linear correlation between alcohol dielectric constants (ε) and gel melting temperatures (T_g) was found. The ^{1}H NMR and FTIR spectroscopic investigations of selected gels reveal the existence of temperature dependent network assembly/dissolution equilibrium. In the ^{1}H NMR spectra of gels only the molecules dissolved in entrapped solvent could be observed. By using an internal standard, the concentration of dissolved gelator molecules could be determined. In FTIR spectra, the bands corresponding to network assembled and dissolved gelator molecules are simultaneously present. This enabled determination of the K_{gel} values by using both methods. From the plots of $\ln K_{gel}$ versus $1/T$, the ΔH_{gel} values of selected gels have been determined ($-\Delta H_{gel}$ in $10-36$ kJ mol^{-1} range) and found to be strongly solvent dependent. The ΔH_{gel} values determined by ^{1}H NMR and FTIR spectroscopy are in excellent agreement. Crystal structures of **2a** and *rac*-**5a** show the presence of organisational motifs and intermolecular interactions in agreement with those in gel fibres elucidated by spectroscopic methods.

Keywords: amino acids · amides · gels · NMR spectroscopy · supramolecular chemistry

Introduction

Successful synthesis of organised supramolecular assemblies is the fundamental step on the way to new materials or functional supramolecular devices.[1–3] Recent reports on a variety of low molecular mass organic molecules, capable of gelatinising various liquids, have attracted considerable attention.[4] Here, gelation represents a macroscopic manifestation of a molecular self-assembly process. The assembly into fibrous supramolecular aggregates leads to formation of a gel network.

However, at the present state of research, it is still hardly possible to predict gelation on the basis of the constitutional and conformational characteristics of the molecule. Considering the structural characteristics of the discovered small organic gelators, two broad families emerge: a) highly lipophilic gelators, represented by steroidal,[5] anthryl[6] or fatty acid[7] derivatives, and b) gelators based on amino acid, urea or other types of functionalities with high hydrogen bonding potential.[8, 9]

We have reported on the gelation properties of bis(leucine) (**1a**) and bis(phenylglycine) (**5a**) oxalyl diamides, which are among the rare gelators with ambidextrous capability to gelatinise both the lipophilic organic solvents and water.[10] In contrast to numerous studies on organic gelators capable of forming gels with lipophilic solvents, the properties of ambidextrous gelators have been less explored. Such a study

[a] Prof. M. Žinić, Dr. J. Makarević, Dr. M. Jokić
Laboratory of Supramolecular and Nucleoside Chemistry
Rudjer Bošković Institute
P.O. Box 180, 10002 Zagreb (Croatia)
Fax: (+385)1-46-80-195
E-mail: zinic@rudjer.irb.hr

[b] Dr. B. Kojić-Prodić, B. Perić
Laboratory for Chemical Crystallography
and Biocrystallography, Rudjer Bošković Institute
P.O. Box 180, 10002 Zagreb (Croatia)

[c] Dr. V. Tomišić
Laboratory of Physical Chemistry
Faculty of Science, University of Zagreb (Croatia)

Supporting information for this article is available on the WWW under http://www.wiley-vch.de/home/chemistry/ or from the author.

  0947-6539/01/0715-3328 $ 17.50+.50/0

may reveal specific organisational motifs that govern gelation of water or lipophilic organic solvents and may shed more light on the gelator–solvent relationship. In this work, we describe a study on gelation properties of a series of bis(amino acid) oxalyl amides. Their derivatives with modified terminal functions (methyl ester, amide) have been also prepared in order to modulate their water/organic solvent gelation preferences. The organisational motifs of such ambidextrous gelator molecules in aqueous and organic gels as well as in the solid state have been studied by TEM, SEM, FTIR, NMR and X-ray structure analysis.

Results

Synthesis: A series of bis[Leu, Val, Ile, Phe, Phg (D-phenylglycine), Trp] oxalyl amides **1a**–**6a** has been prepared by condensation of the respective amino acid with oxalyl chloride (biphasic CH_2Cl_2/water system, aqueous KOH). The method also enables simultaneous preparation of racemic and *meso*-oxalyl amides starting from racemic amino acids.[10] The methyl ester derivatives **1b**–**5b** were prepared from the respective amino acid methyl esters and oxalyl chloride in dichloromethane. The diamide derivatives **1c**–**5c** were obtained by ammonolysis of the respective methyl ester derivatives.

Abstract in Croatian: *Bis(LeuOH) (**1a**), bis(ValOH) (**2a**) i bis(PhgOH) (**5a**) (Phg označava (R)-fenilglicin) oksal amidi su efikasni gelatori male molekulske mase koji geliraju različita organska otapala, njihove smjese kao i vodu te smjese voda/DMSO i voda/DMF. Njihovo uređenje u hidro- gelskim mrežama prvenstveno određuju međumolekulske lipofilne interakcije dok je uređenje u organskim gelovima određeno tvorbom međumolekulskih vodikovih veza. Gelovi su većinom termoreverzibilni i stabilni kroz više mjeseci. Međutim, **2a** tvori nestabilne gelove s organskim otapalima koji starenjem prelaze u različite kristalne oblike. Za gelove nekih nižih alkohola s **1a** utvrđeno je da postoji linearna međuovisnost dielektrične konstante (ε) alkohola i temperaturne točke taljenja gela (T_g). Proučavanje gelova ^1H NMR i FTIR spektroskopijom otkriva temperaturno ovisnu ravnotežu između gelske mreže i otopine gelatora u gelskoj tekućini. NMR spektar gela odgovara samo molekulama gelatora otopljenim u gelskoj tekućini; upotrebom unutarnjeg standarda može se odrediti njegova koncentracija. U FTIR spektrima gela prisutne su istovremeno vrpce gelatora organiziranog u gelskoj mreži i vrpce gelatora otopljenog u gelskoj tekućini. Ovo omogućava određivanje K_{gel} NMR i FTIR metodama. Iz linearne ovisnosti $\ln K_{gel}$ o 1/T određene su ΔH_{gel} vrijednosti nekih gelova ($-\Delta H_{gel}$ u rasponu od 10–36 kJ mol^{-1}) koje značajno ovise o otapalu. Vrijednosti za ΔH_{gel} dobivene NMR i FTIR metodama se potpuno slažu. Kristalne strukture **2a** i rac-**5a** određene rentgenskom strukturnom analizom pokazuju motive uređenja i intermolekulske interakcije slične onima u gelskim nitima koje su utvrđene spektroskopskim metodama.*

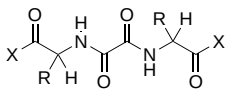

(*S*,*S*)-**1a**: R = $CH_2CH(CH_3)_2$; X = OH
(*S*,*S*)-**1b**: R = $CH_2CH(CH_3)_2$; X = OCH_3
(*S*,*S*)-**1c**: R = $CH_2CH(CH_3)_2$; X = NH_2

(*S*,*S*)-**2a**: R = $CH(CH_3)_2$; X = OH
(*S*,*S*)-**2b**: R = $CH(CH_3)_2$; X = OCH_3
(*S*,*S*)-**2c**: R = $CH(CH_3)_2$; X = NH_2

(*S*,*S*)-**3a**: R = $CH(CH_3)CH_2CH_3$; X = OH
(*S*,*S*)-**3b**: R = $CH(CH_3)CH_2CH_3$; X = OCH_3
(*S*,*S*)-**3c**: R = $CH(CH_3)CH_2CH_3$; X = NH_2

(*S*,*S*)-**4a**: R = CH_2Ph; X = OH
(*S*,*S*)-**4b**: R = CH_2Ph; X = OCH_3
(*S*,*S*)-**4c**: R = CH_2Ph; X = NH_2

(*R*,*R*)-**5a**: R = Ph; X = OH
(*R*,*R*)-**5b**: R = Ph; X = OCH_3
(*R*,*R*)-**5c**: R = Ph; X = NH_2

(*S*,*S*)-**6a**: R = CH_2Indolyl; X = OH

Gelation experiments: The results of gelation experiments with various solvents and solvent mixtures are given in Table 1. Gelation efficiency is expressed as the maximal solvent/gelator molar ratio (S_{max}) corresponding formally to the number of solvent molecules immobilised by a single gelator molecule. Due to insufficient solubility of this type of compound in most of the common organic solvents except the most polar solvents, such as DMSO, DMF, MeOH, the gelation of solvent mixtures was investigated. The gelation procedure is reminiscent of two-solvent recrystallization in a way that DMSO, DMF or any other polar solvent as the minor solubilising component and a second solvent of lower polarity in excess were used. It was found that most of the examined gelators are capable of gelatinising some pure solvents and various solvent mixtures, including water/DMSO and water/DMF (Table 1). In most cases, thermally reversible gels were formed. As reported previously, the racemates and *meso*-diastereoisomers lack gelation ability.[10] The Leu derivative **1a** gives the most stable gels; if kept in closed tubes the

Table 1. Gelation of water/DMSO, water/DMF and other solvents and solvent mixtures[a] by 10 mg of oxalyl bis(amino acid) derivatives expressed as maximal solvent/gelator molar ratios (S_{max}).

Compound	S_{max} H_2O/DMSO *v*/*v*	S_{max} H_2O/DMF *v*/*v*	S_{max}, solvent system (solvent ratio)
1a	1278; (5.0)	434; (4.0)	1760 water; 556 EtOH; 279, dioxane; 156 THF, 113 EtOAc; 150 acetone
1c	ng[b]	ng	2247 CH_2Cl_2/MeOH (1.9); 1837 CH_2Cl_2/acetone (1.1)
2a	ng	ng	1460 heptane/EtOAc (3.6); 2265 cyclohexane/acetone (9.1); 1231 $CHCl_3/CH_3CN$ (5.03)
2c	ng	2158; (5.0)	202 DMSO; 194 DMF/ether (2.5)
3a	ng	ng	225 MeOH/dioxane (4.8); 243 THF; 304 THF/hexane (3.9); 103, CH_2Cl_2/MeOH (10.4); 262 EtOAc/hexane (3.4)
5a	3540; (19.0)	1723; (11.4)	1786 water; 1678 dioxane

[a] The following laboratory solvents have been tested for gelation: heptane, hexane, petroleum ether, cyclohexane, CH_2Cl_2, $CHCl_3$, Et_2O, THF, dioxane, acetone, EtOAc, EtOH, MeOH. [b] No gelation, crystallisation or dissolution occurred.

aqueous and EtOH gels remained unchanged for many months. In contrast to dicarboxylic acid derivatives **1a**–**3a** and **5a** the methyl esters **1b**–**5b** lack gelation of the same solvent systems. Among the members of the terminal carboxamide series **1c**–**5c** only **1c** and **5c** exhibited gelation while the other members tend to crystallise.

Gelation of alcohols by 1a—The T_g/alcohol dielectric constant correlation: The Leu derivative **1a** gave excellent thermoreversible gelation of various alcohols (Table 2). Thermal stabilities of the gels were determined by heating tube samples in the thermostated bath until tube inversion showed that the gel had melted.

Table 2. Gelation of alcohols by **1a** expressed as maximal solvent/gelator molar ratio S_{max}[a] and T_g values of 0.043 mol dm^{-3} gels.

Solvent	S_{max}	T_g [°C]	Solvent	S_{max}	T_g [°C]
methanol	–	< 0	1-hexanol	466	130
ethanol	855	45	cyclohexanol	1350	104
1-propanol	1252	75	1-heptanol	461	102
2-propanol	428	74	1-octanol	297	103
1-butanol	1480	97	1-nonanol	575	103
isobutanol	507	53	1-decanol	560	116
2-butanol	1130	95	1-dodecanol	560	118
2-butenol	862	74	2-phenyl-etanol	1540	138
1-pentanol	292	107	1,4-butanediol	283	86
2-methyl-2-butanol	1069	103	1,2,3-propane-triol	687	54
3-methyl-butanol	614	108			

[a] Determined for 10 mg of **1a**.

We found that the T_g values of gels with (C_1–C_6) *n*-alcohols, but also of some cyclic and branched C_3–C_6 alcohols, show linear correlation ($r^2 > 0.99$) with alcohol dielectric constants (ε), being in the range from 13 (1-hexanol) to 32.7 (MeOH) (Figure 1a). However, for the gels with higher (C_7–C_{12}) alcohol homologues ε values between 11.75 and 5.82 were observed as well as no linear T_g/ε correlation at all for *i*BuOH and 2-methyl-2-butanol gels (Figure 1b); in each case much lower T_g values than expected were measured on the basis of their ε values.

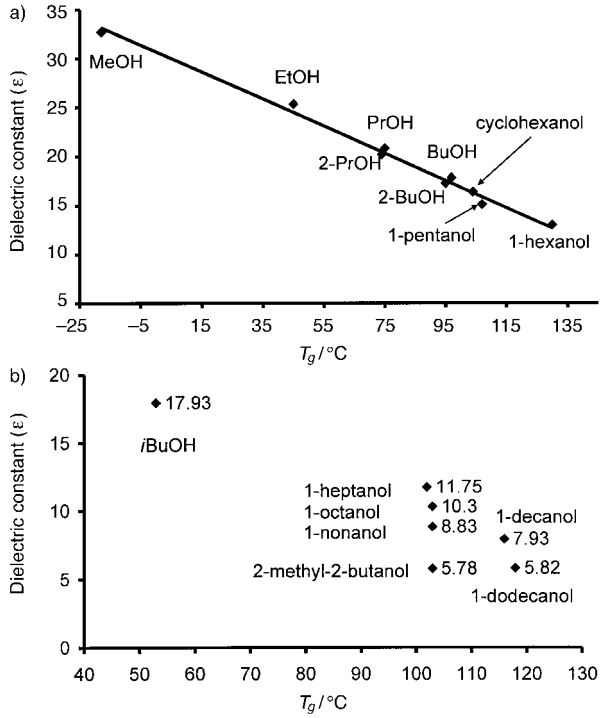

Figure 1. a) Linear alcohol dielectric constant (ε)/gel melting temperature (T_g, °C) correlation for some **1a**/alcohol gels. b) ε and T_g values of some higher and branched alcohol gels.

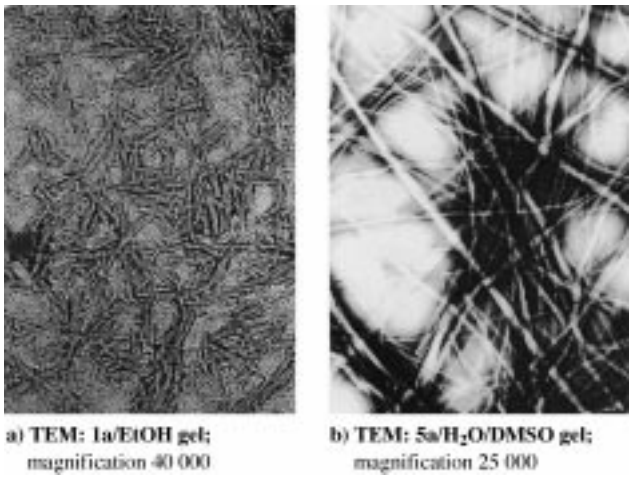

Figure 2. TEM images of selected **1a** and **5a** gels.

TEM and SEM investigations: The TEM micrographs of **1a**/EtOH (Figure 2a) and **1a**/dioxane (not shown) gels show the presence of very dense networks, the latter consisting of somewhat thicker fibres than the former. The TEM image of **5a**/DMSO/water gel (Figure 2b) reveals a less dense network containing straight and interwound fibres of larger diameters. The smallest fibre diameters found by TEM are in the range of 10–20 nm.

The Val derivative **2a** represents a special case of this type of gelators, as it gives unstable gels with organic solvents which upon ageing transform into a variety of crystalline shapes. In contrast to other gelators of the same series, **2a** is soluble in EtOAc and acetone and gives gels upon addition of the second highly lipophilic solvent such as heptane, hexane, petroleum ether or cyclohexane to the solution. The **2a** EtOAc/heptane gel, upon ageing at room temperature, transforms to crystalline fibres and then first to smaller and then larger crystalline tubes (Figure 3, top left and Figure 1 Supporting Information). In another sample of **2a** EtOAc/heptane gel, besides fibres, crystalline spheres of 40–60 μm diameter were observed by SEM (Figure 3, top right). From the acetone/heptane gel, the crystals of **2a** together with smaller crystalline spheres of 1–3 μm were formed (Figure 1, Supporting Information). The **2a** acetone/cyclohexane gel, upon ageing at +4 °C, transforms to long fibres, macrocycles and catenanes of micrometer-dimensions, observable under optical microscope with crossed polarizers (Figure 3, bottom row); the latter shows optical anisotropy of ordered aggregates. The observed transformations were found to be extremely sensitive to the experimental conditions (composition of solvent mixture, concentration and temperature regime), and those leading to formation of crystalline tubes

0947-6539/01/0715-3330 $ 17.50+.50/0 *Chem. Eur. J.* **2001**, *7*, No. 15

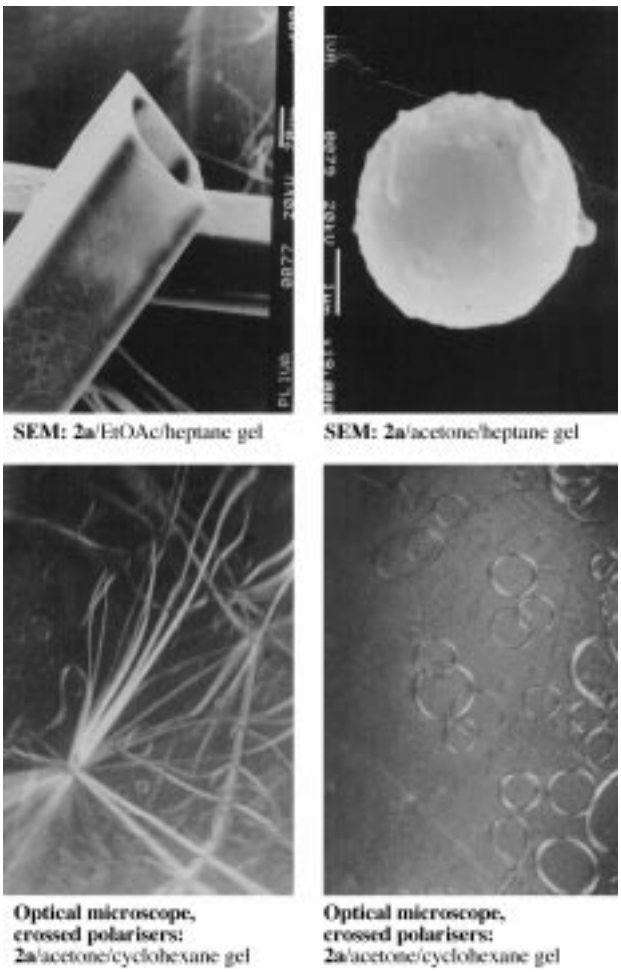

Figure 3. Top row: SEM images showing various crystalline shapes formed from **2a** gels. Bottom row: shapes observed under optical microscope with crossed polarizers.

cannot be controlled at present. Ageing of **2a** EtOAc/petroleum ether gel produced crystals of good quality for X-ray analysis; the crystal structure was determined (see the Section on X-ray analysis).

FTIR investigations of the hydrogen bonding interactions: Characteristic FTIR bands of selected xerogels are listed in Table 3. The positions of **1a**- and **5a**-NH, -amide I and -amide II bands in the xerogels obtained from polar PrOH, less polar EtOAc/CH_2Cl_2 and highly polar DMSO/water gels are in accord with the intermolecular oxalyl amide – oxalyl amide hydrogen bonding in gel fibres formed in each medium. The carboxyl CO stretching bands appear in the 1720 – 1728 cm^{-1} range which is indicative of the lateral type of hydrogen bonding found earlier in some polycarboxylic acid derivatives.[11] Thus, in highly polar water/DMSO or water/DMF gels as well as in those formed with lipophilic organic solvents, the organisations in fibres are based on intermolecular hydrogen bonding, involving both the oxalyl amide and carboxyl groups. The FTIR of diluted (10^{-3} mol dm^{-3}) solution of **2a** in CH_2Cl_2 identifies the position of bands belonging to non-hydrogen bonded functionalities. In the spectrum of diluted **2a**/dioxane/CH_2Cl_2 (solvents 1:12) gel the bands of hydrogen bonded and free functionalities of **2a** are present simultaneously corresponding to gel network assembled and dissolved (free or weakly hydrogen bonded) **2a** molecules, respectively (Table 3).

Table 3. Characteristic FTIR bands ($\tilde{\nu}$, cm^{-1}) of selected gels, xerogels and **2a** solution.

Xerogel solvent[a]	NH	CO(OH)	Amide I	Amide II
2a EtOAc/CH_2Cl_2 1:1	3260	1730	1668	1515
2a[b] dioxane/CH_2Cl_2 1:12	3395; 3250	1731 – 1723	1690; 1670	1515; 1505
2a[c] CH_2Cl_2	3398	1726	1690	1505
1a PrOH	3300	1728, 1738 1745	1658, 1664	1525
1a EtOAc	3280	1725, 1745	1663	1515
1a DMSO/water	3300	1720, 1729	1658	1515
5a DMSO/water	3305	1720, 1728 1736, 1745	1655	1515

[a] Solvent or solvent mixture used for preparation of the gel. [b] Dilute gel of **2a** with simultaneously present bands of network assembled and dissolved **2a**. [c] Dilute (10^{-3} mol dm^{-3}) solution of **2a** in CH_2Cl_2.

The temperature dependent FTIR spectra of **2a**/CH_3CN/$CHCl_3$ gel ($T_g = 41\,^{\circ}C$) were measured in a 26 – 42 °C temperature range (Figure 4). By temperature increase from 26 °C (gel; the bands of network assembled (ass.) and dissolved (diss.) **2a** simultaneously present: $\tilde{\nu}$, cm^{-1}: 3393 diss. and 3245 ass. NH; 1744 diss. and 1728 ass. CO(OH); 1688 diss. and 1666; 1653 ass. amide I) the bands corresponding to assembled molecules decrease while those corresponding to dissolved molecules increase until in the solution spectrum at 42 °C only the latter bands remain. The presence of several isosbestic points common for two types of spectroscopically distinguishable species at equilibrium can be observed; in this case the gel network assembly and weakly aggregated **2a** molecules present in the entrapped solution. The spectral changes are fully reversible upon cooling of the solution to gel. Using the concentration of **2a** (c_{tot}) and the intensities of amide I or carboxylic carbonyl bands belonging to assembled and dissolved **2a** molecules the ΔH_{gel} of -29 (± 2) kJ mol^{-1} was determined from $\ln K_d$ versus $1/T$ plot (Figure 4, bottom; see next Section for definitions).

^{1}H NMR investigations—Determination of K_{gel} and ΔH_{gel}: Derivatives **1a**, **2a** and **5a** form gels with some common NMR solvents, which allowed ^{1}H NMR studies of these gels to be performed. The bis(ValOH)-derivative **2a** (2.75 mg) forms gel with the CD_3CN (0.1 mL)/$CDCl_3$ (0.5 mL) mixture. The gel spectrum and the spectrum of the solution obtained by heating the same sample to 55 °C are very similar (only slight chemical shift and signal width differences are observable), except for significantly different intensities of the solvent signal (non-deuterated residue of CD_3CN, $\delta = 1.992$). The

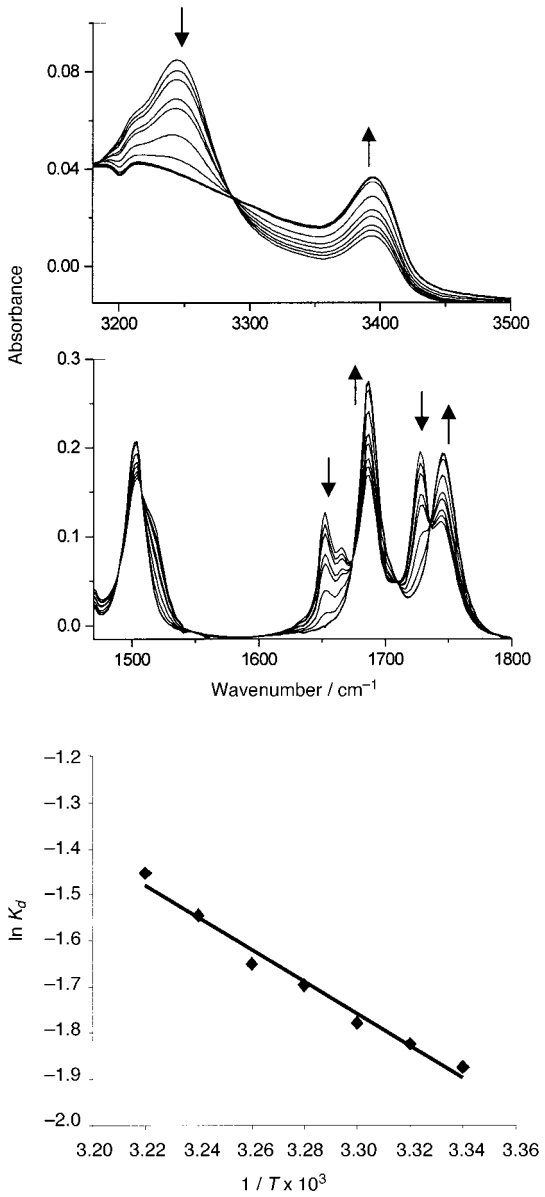

Figure 4. Temperature dependent (26–41 °C) FTIR spectra of **2a**/CH_3CN/$CHCl_3$ (2.5:1 *v*/*v*) gel. Intensity changes of NH, CO(OH), amide I and amide II bands by temperature increase are indicated by arrows (top). $\ln K_d$ versus $1/T$ plot used for calulation of ΔH_{gel} (bottom).

solvent signal intensity in the gel spectrum appears considerably higher than that in the solution spectrum (Figure 2, Supporting Information); this corresponds to the lower **2a** concentration in the gel than in the solution. As pointed out recently,[8d] the signals of the gelator molecules assembled in the rigid gel network are expected to broaden to the point of non-observability as a result of long correlation times. Therefore, the observed gel spectrum should correspond to the **2a** molecules (or smaller assemblies) dissolved in the entrapped solvent.[12] The ^{1}H NMR spectra of the gel with the known total concentration (c_{tot}) of **2a** were recorded at different temperatures in the presence of the known concentration of 1,1,2,2-tetrachloroethane ($\delta = 6.43$) used as internal standard. By temperature increase, the internal standard to NH and C*H signal intensity ratios (I_{st}/I_{Hi}) significantly decreased in accord with the increased concentration of **2a** molecules in the entraped solvent, apparently formed by dissociation of the gel network. The changes of the ratio ceased at temperatures close to T_g (T_g of 44 °C determined by tube inversion method) (Figure 5a). The curves in Figure 5a confirm the existence of the temperature dependent equilibrium between the gel network assembly and **2a** molecules dissolved in the entrapped solvent. The existence of the same assembly/dissolution equilibrium was also observed by the temperature dependent FTIR (Figure 4). From the known concentrations of the internal standard and **2a** (c_{tot}), the concentrations of the dissolved (c_d) and the assembled ($c_{tot} - c_d$) gelator molecules at each temperature can be calculated.

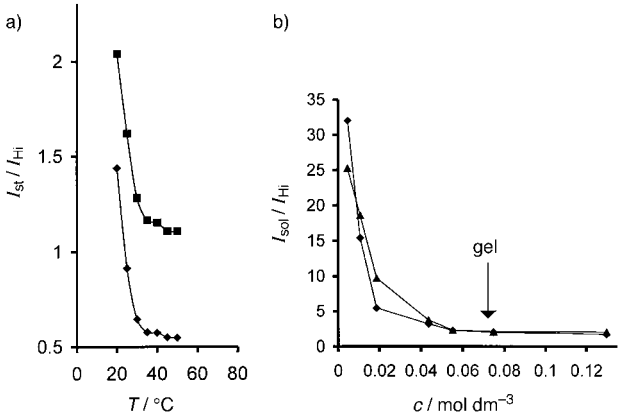

Figure 5. a) Changes of the standard ($Cl_2CHCHCl_2$) to H_i intensity ratios (I_{st}/I_{Hi}) versus temperature:(■) H_i = C*H; (◆) H_i = NH. b) Changes of solvent (CD_3CN) to H_i signal intensity ratios (I_{sol}/I_{Hi}) with concentration of **2a**: C*H (◆), NH (▲).

We also examined the dependence of the solvent to H_i intensity ratio (I_{sol}/I_{Hi}) on the total **2a** concentration (c_{tot} in the range of 0.01–0.13 mol dm^{-3}) covering the solution and gel phases; at $c_{tot} = 0.074$ mol dm^{-3}, formation of gel was observed (Figure 5b). At a low concentration range, steep and practically linear decrease of the I_{sol}/I_{Hi} ratio was observed. In the pre-gelation state (0.02–0.04 mol dm^{-3} concentration range) strong curvature is observed. The latter can be explained by formation of large gelator assemblies still present in the solution; the existence of large assemblies diminishes gelator signal intensities (I_{Hi}) due to prolonged correlation times. The increase of the **2a** concentration above the gelation point observed at 0.074 mol dm^{-3} does not change the I_{sol}/I_{Hi} ratio, and implies a constant concentration of gelator molecules in the entrapped solvent. The latter suggests that the equilibrium is determined by c_d. Hence, the dissolution and gelation constants may be defined as $K_d = [c_d]$ and $K_{gel} = 1/[c_d]$. Determination of K_{gel} (or K_d) by ^{1}H NMR spectroscopy at different temperatures allows calculation of ΔH_{gel} (or ΔH_d) from the $\ln K_{gel}$ versus $1/T$ plots according to the following Equation (1):

$$\ln K_{gel} = \frac{-\Delta H_{gel}}{R} \cdot \frac{1}{T} + C \qquad (1)$$

Using this approach,[13] the ΔH_{gel} values were determined for **1a**/[D_6]EtOH, **1a**/D_2O/[D_6]DMSO [internal standard sodium 3-(trimethylsilyl)-propanesulfonate, $\delta = 0.00$ used for D_2O containing gels], **2a**/CD_3CN/$CDCl_3$ and **5a**/D_2O/DMSO gels.

0947-6539/01/0715-3332 $ 17.50+.50/0 *Chem. Eur. J.* **2001**, *7*, No. 15

Plots of log K_d against $1/T$ gave satisfactory straight lines ($r^2 = 0.97-0.99$; Figure 6). The ΔH_{gel} values determined are collected in Table 4.

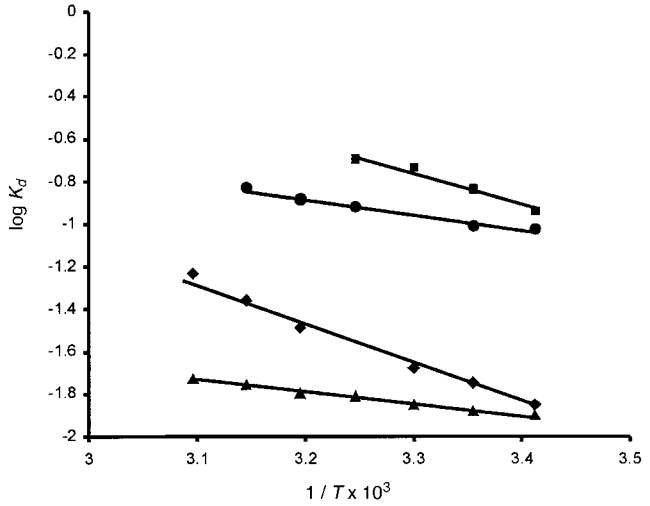

Figure 6. Plots of log K_d versus $1/T$ of the gels (compd., solvent mixture v/v): (●) **1a**/D_2O/[D_6]DMSO (3.3:1); (◆) **1a**/[D_6]EtOH; (■) **2a**/CD_3CN/$CDCl_3$ (2.5:1); (▲) **5a**/D_2O/[D_6]DMSO (2:1).

Temperature and concentration dependent ^{1}H NMR spectra: Monitoring of a gelator's chemical shift changes in ^{1}H NMR spectra by variation of temperature and concentration can provide valuable information on the organisation of dissolved gelator assemblies[12] present at equilibrium with the gel network or those present at pre-gelation concentrations (defined as concentration range lower than the critical gelation concentration). The chemical shift changes in the spectra of **2a**/CD_3CN/$CDCl_3$ gel upon temperature increase are shown in Figure 7a–d; the asymmetric carbon-H (C*H), methine and methyl protons very slightly shift downfield ($\Delta\delta = 0.009-0.020$ ppm; Figure 7b–d) while NH protons of the oxalyl amide fragments shift upfield ($\Delta\delta = 0.020$ ppm; Figure 7a). The opposite direction of NH shifts (downfield; $\Delta\delta = 0.040$ ppm) was observed by increasing the concentration of **2a** in the same solvent mixture until the critical gelation concentration of 0.074 mol dm^{-3} was reached (Figure 7e).

Molecular and crystal structures of 2a, and (±)-5a: The crystals of **2a** were grown directly from the EtOAc/petroleum ether gel.

Table 4. ΔH_{gel}, total gelator concentrations (c_{tot}) and the mol fraction (x) percentages of the network assembled and dissolved gelator molecules at 20 °C.

Gelator; solvent (solvent ratio v/v)	$c_{tot} \times 10^2$ mol dm^{-3}	x [%] assembled[a]	x [%] dissolved[a]	$-\Delta H_{gel}$[b] [kJ mol^{-1}]
1a D_2O/[D_6]DMSO (3.3:1)	7.25	80	20	36 (±2)
1a [D_6]EtOH	15.37	38	62	14 (±1)
2a CD_3CN/$CDCl_3$ (2.5:1)	23.69	51	49	29 (±3)
5a D_2O/[D_6]DMSO (2:1)	2.25	44	56	10 (±1)

[a] Calculated for gels at 20 °C at given c_{tot}. The term dissolved denotes gelator molecules present in the gel liquid detectable by ^{1}H NMR spectroscopy. [b] Determined from log K_d versus $1/T$ plots; standard errors given in parentheses.

The organisation in the crystalline state may shed light on organisation in gel fibres. Also the organisation in the crystals of non-gelling (±)-**5a** grown from water/DMSO solvent system may resemble the organisation in fibres of (*R*,*R*)-**5a** gel formed with the same mixture of solvents.

Molecular structures of *N*,*N*-oxalyl-bis(ValOH) (**2a**, Figure 8), and racemic *N*,*N*-oxalyl-bis(PhgOH) [(±)-**5a**,

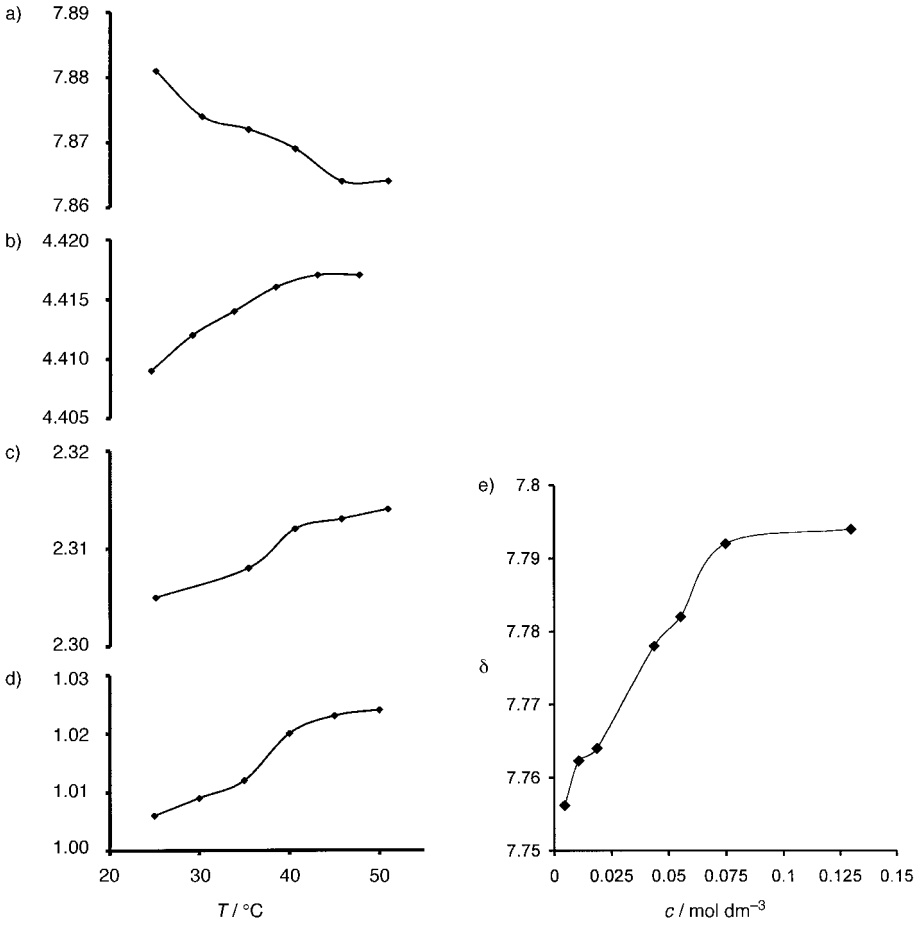

Figure 7. Changes of selected **2a** chemical shifts (δ_{Hi}) versusu temperature in ^{1}H NMR spectra of **2a**/CD_3CN/$CDCl_3$ gel: a) NH; b) CH; c) CH_3; d) C*H (left); e) concentration dependent δ_{NH}.

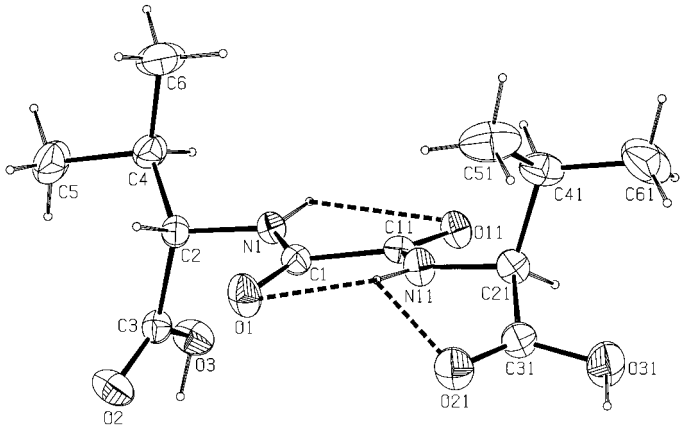

Figure 8. ORTEP drawing of **2a** with the atom numbering and intramolecular hydrogen bonds. Thermal ellipsoids are scaled at 30% probability.

Figure 9] are defined by a set of torsion angles (Table 5) assigned analogous to the peptide nomenclature.[16] Their values are within regions of the Ramachandran diagram (Φ versus Ψ plot). Detected conformational differences of two amino acid residues within the molecule are caused by packing effects generated by hydrogen bonding, CH$\cdots\pi$, and $\pi\cdots\pi$ interactions [(±)-**5a**].

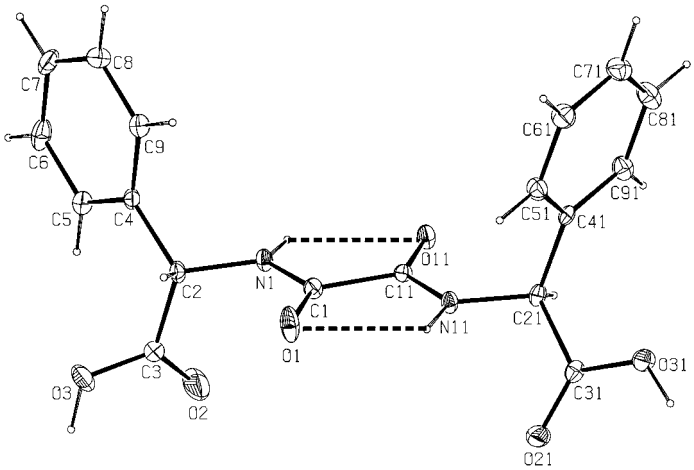

Figure 9. ORTEP drawing of (±)-**5a** with the atom numbering and intramolecular hydrogen bonds. Thermal ellipsoids are scaled at 30% probability.

Table 5. Selected torsional angles of **2a** and (±)-**5a** [°].

		2a	(±)-**5a**
ω	C11-C1-N1-C2	−179.3(2)	178.2(1)
	C1-C11-N11-C21	176.7(2)	179.4(1)
ϕ	C1-N1-C2-C3	−85.8(2)	−89.6(2)
	C11-N11-C21-C31	−146.4(2)	−146.2(2)
ψ	N1-C2-C3-O3[a]	−74.1(2)	159.8(2)
	N11-C21-C31-O31[a]	160.2(2)	−151.7(2)
χ	N1-C2-C4-C5	175.6(2)	116.4(2)
	N11-C21-C41-C51	69.1(3)	47.3(3)

[a] The torsion angles $\omega \rightarrow \chi$ are assigned analogously to the nomenclature of peptides.[29]

The molecular structure of the valine analogue (**2a**) reveals non-planar oxalyl amide bridge. The values of torsion angles involving this moiety illustrate a deviation: O1=C1−C11=O11 is 166.9(2)° and N1−C1−C11−N11 is 169.2(2)°. According to the Csp^2 hybridisation, the group should be planar as confirmed in the structure of (±)-**5a** and other retropeptides of this kind.[17–19] The out-of-plane distorsion of carboxamide groups about C1−C11 bond can be explained by their asymmetrical function in hydrogen bonding (details to be discussed in the next paragraph).

Crystal packing and hydrogen bonding: The crystal packing of **2a** does not include a solvent. A structural unit is a dimer formed by the intermolecular N1-H1$\cdots$O11 hydrogen bonds between oxalyl amide groups, which built a non-planar ten-membered ring, defined in the graph-set notation as $R_2^2(10)$[20] (Table 6, Figure 10a). Such dimers are connected by carboxyl and oxalyl amide groups through hydrogen bonds O3-H3$\cdots$O11 [$C(8)$] into two infinite chains forming a double helix running along a two-fold axis in the direction of *c* (Figure 10b). The infinite helixes are interlinked by hydrogen bonds between carboxyl groups O31-H31$\cdots$O2 in the plane perpendicular to the two-fold axis and a three-dimensional network was obtained (Figure 10c). In addition to intermolecular hydrogen bonds, there are three intramolecular hydrogen bonds. The atom N11 acts as a proton donor to two intramolecular hydrogen bonds (N11-H11$\cdots$O1 and N11-H11$\cdots$O21) whereas the amide group of N1 participates in intramolecular (N1-H1$\cdots$O11) and intermolecular (N1-H1$\cdots$O11[c] in Table 6) hydrogen bonds. Two of these hydrogen bonds are of a pseudo-C_5 type typical of retropeptides.

The crystal structure of *rac*-**5a** reveals the most complex pattern. The basic building block is a centrosymmetric dimer (Figure 11a, Table 7) generated by hydrogen bonds between crystalline water molecules and carboxyl group (O3-H3$\cdots$O4 and O4-H41$\cdots$O21). Necessarily, the centrosymmetric ring structure includes molecules of opposite chirality. The ring structures are stacked one above the other and connected into infinite tunnels along the *a* axis (Figure 11c) through hydrogen bonds N1-H1$\cdots$O1 and N11-H11$\cdots$O1 of the oxalyl amide groups (Table 7). These tunnels are occupied by disordered water molecules. Each of the two intramolecular hydrogen bonds N11-H11$\cdots$O1 and N1-H1$\cdots$O11 of the oxalyl amide groups generates the pseudo-C_5 pattern. Hydrogen bonds O3-H3$\cdots$O4 and O4-H42$\cdots$O31 (Table 7, Figure 10c) form an infinite chain [$C(13)$] along the *b* axis and thus connects molecules of the same chirality. Around the inversion centre two carboxyl groups are involved into a tandem hydrogen bond, O31-H31$\cdots$O31 (Table 7) forming a four-membered ring defined in the graph-set notation as $R_2^2(4)$. This hydrogen bond connects layers of opposite chirality. The packing of this racemic compound is composed of separated enantiomeric layers which are connected through hydrogen bonds with water molecules. Hydrophilic layers are separated by phenyl groups involved in a $\pi\cdots\pi$ interactions (interplanar distance of translated phenyl rings 3.327 Å). Contribution to weak interactions are from CH$\cdots\pi$ contacts; molecules related by symmetry inversion operation realise contact distance of 3.041 Å between C_g (C41 → C91

  0947-6539/01/0715-3334 $ 17.50+.50/0 *Chem. Eur. J.* **2001**, *7*, No. 15

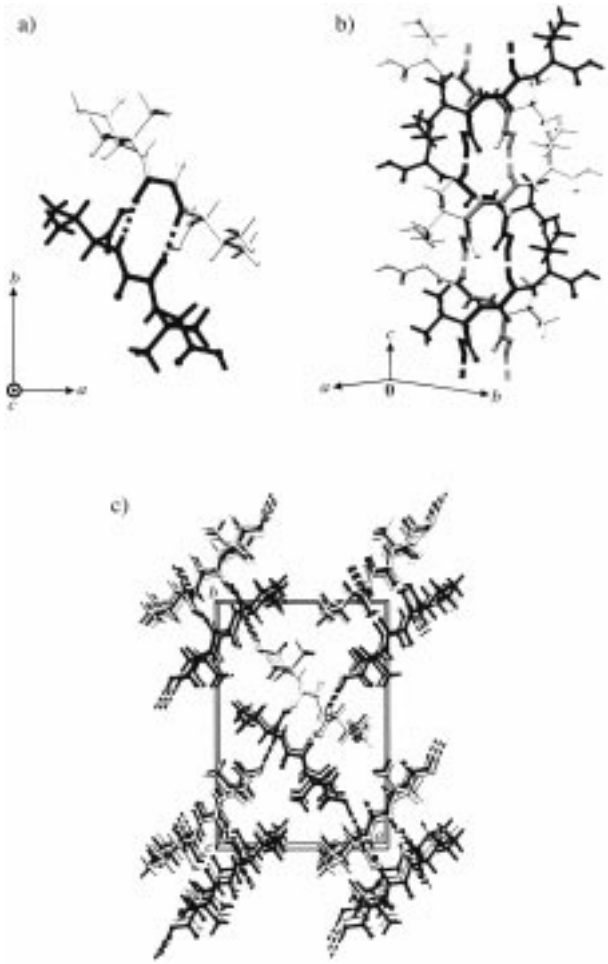

Figure 10. a) In the crystal structure of **2a** dimers are formed through hydrogen bonds between the oxalyl amide groups [$R_2^2(10)$], a view along a two-fold axis is shown; b) two infinite chains [$C(8)$] (shown in light and dark gray) formed from connected dimers through hydrogen bonds between carboxylic acid and oxalyl amide groups generate the double helix running along c; c) a three-dimensional network is realized by interlinked double helices by hydrogen bonds between carboxyl groups.

Table 6. Hydrogen bond geometry in the crystal structure of **2a**.

	D–H [Å]	H···A [Å]	D···A [Å]	D-H···A [°]	Graph-set descriptor
O3-H3···O11[a]	0.90(4)	1.87(4)	2.738(2)	161(3)	$C(8)$
O31-H31···O2[b]	0.85(4)	1.87(4)	2.675(3)	157(4)	$C(11)$
N1-H1···O11[c]	0.82(3)	2.21(3)	3.017(2)	171(3)	$R_2^2(10)$
N11-H11···O1	0.82(3)	2.31(3)	2.675(3)	108(3)	$S(5)$
N1-H1···O11	0.82(3)	2.43(3)	2.750(2)	105(2)	$S(5)$
N11-H11···O21	0.82(3)	2.41(3)	2.702(3)	102(3)	$S(5)$

[a] $-x, -y, -1+z$; [b] $-\frac{1}{2}+x, \frac{1}{2}-y, 1-z$; [c] $-x, -y, z$.

ring)···H7-C7 (C4 → C9 ring). Fowler and Lauher[21] recognised the formation of dimers in the racemic crystals around the centre of symmetry instead of the typical α network characteristic of enantiomeric species. However, due to the dislocation of the inversion centre from the plane of oxalyl amide group, translation operation allows formation of an infinite α network including molecules of the same chirality, which are a fragment of β network, as we observed in the crystal structure of (±)-**5a**.

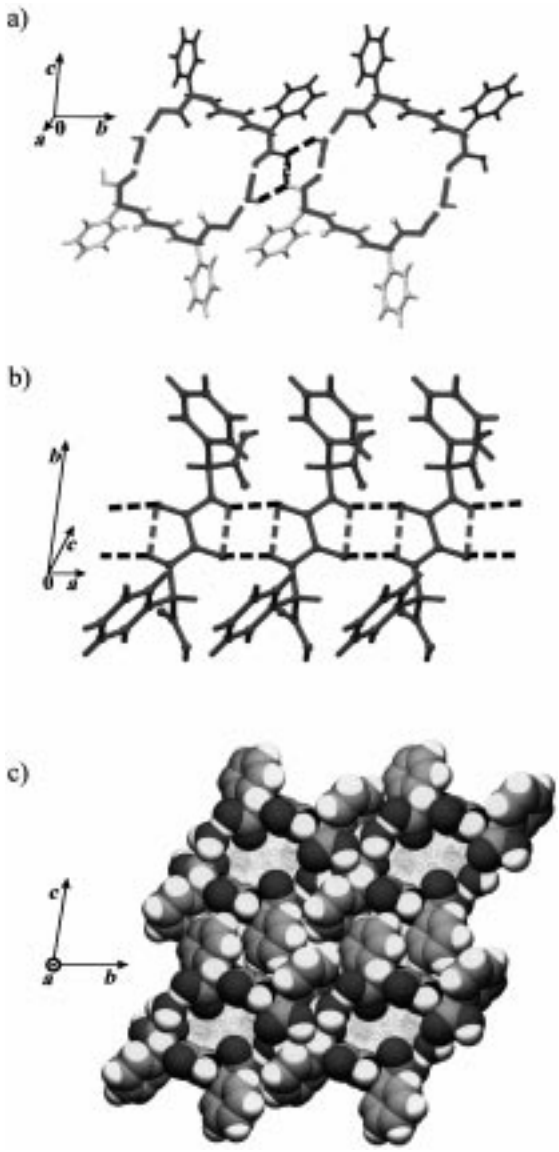

Figure 11. a) A basic building block of the crystal packing of (±)-**5a** is a centrosymmetric dimer formed by hydrogen bonds between crystalline water molecules and carboxyl groups; dimers are connected through hydrogen bonds between water molecules and carboxyl group forming an infinite chain of the molecules of the same chirality along b whereas tandem hydrogen bonds, involving carboxyl groups around the inversion centre, join molecules of opposite chiralty along c. b) Hydrogen bonds between oxalyl amide groups, which form an ladder pattern, connect dimers along a closing channels occupied by disordered water molecules. c) A spherical presentation of the crystal packing with the holes occupied by disordered water molecules; residual electron density is shown.

Table 7. Hydrogen bond geometry in the crystal structure of (±)-**5a**.

	D–H [Å]	H···A [Å]	D···A [Å]	D-H···A [°]	graph-set descriptor
O3-H3···O4	0.98(4)	1.58(4)	2.556(2)	175(4)	D
O4-H41···O21[a]	1.01(4)	1.73(4)	2.736(3)	178(4)	D
O4-H42···O31[b]	0.82(4)	2.20(4)	2.850(3)	136(4)	D
O31-H31···O31[c]	0.87(8)	1.66(8)	2.477(3)	156(8)	$R_2^2(4)$
N1-H1···O1[d]	0.86(3)	2.13(3)	2.946(3)	158(2)	$C(4)$
N11-H11···O11[e]	0.85(3)	2.16(3)	2.924(3)	150(2)	$C(4)$
N11-H11···O1	0.85(3)	2.29(3)	2.688(2)	109(2)	$S(5)$
N1-H1···O11	0.86(3)	2.34(3)	2.724(2)	108(2)	$S(5)$

[a] $2-x, 1-y, -z$; [b] $x, -1+y, z$; [c] $2-x, 2-y, -z$; [d] $-1+x, y, z$; [e] $1+x, y, z$.

Discussion

Gelation of water and water containing solvent mixtures: Among the bis(amino acid) oxalyl amide gelators synthesised the Leu (**1a**) and Phg (**5a**) derivatives exhibited excellent gelation in water and water/DMSO or water/DMF mixtures (Table 1). In comparison to **1a**, the Val-derivative **2a** and Ile-derivative **3a** were found unable to form gels with water or any of the examined water containing solvent mixtures. Also, in contrast to **5a**, which efficiently gelatinised water, the Phe-derivative **4a** and Trp-derivative **6a** failed to form gels. Such a structure–gelation analysis suggests that gelation of water containing systems strongly depends on the type of lipophilic substituents on asymmetric carbons, with other structural fragments being identical for gelling and non-gelling oxalyl amide derivatives.

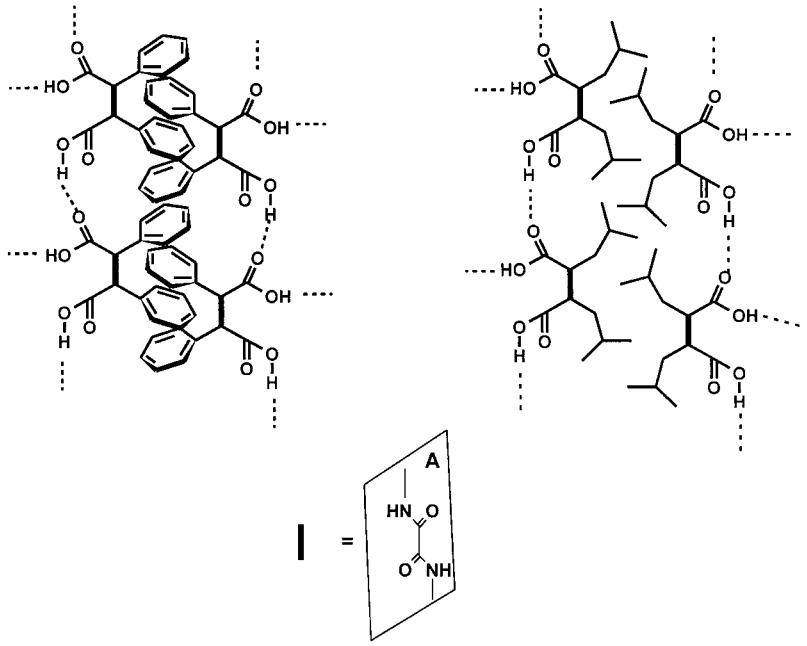

Figure 12. Schematic presentation of **1a** and **5a** organisation in hydrogel fibers based on phenyl stacking and dispersive and hydrophobic interactions. Thick lines denote oxalyl amide fragments laying in the plane *A* perpendicular to the plane of drawing. Intermolecular hydrogen bonding between self-complementary oxalyl amide units in plane *A* and lateral hydrogen bonding between carboxylic groups is indicated.

In a previous communication[10] we postulated the primary association of **5a** in water (Figure 12), based on fluorescence results which confirmed formation of the intermolecularly Ph–Ph stacked assemblies of **5a**. The concentration dependent UV spectra (2.5×10^{-5}–1.1×10^{-3} mol dm^{-3} concentration range of **5a** in water/DMSO 4.8:1 solvent mixture) revealed strong hypochromicity effects (65%, above 0.4×10^{-3} mol dm^{-3}) also in accord with formation of Ph–Ph stacked associates in solution (Figure 2, Supporting Information). The ^{1}H NMR spectra for the **5a**/D_2O/DMSO (3:1) gel are in accord with fluorescence and UV observations; the analysis of chemical shifts ($\Delta\delta_{Ph}$ and $\Delta\delta_{C^*H}$) in the temperature dependent spectra revealed deshielding effects with temperature increase (20 °C, gel, $\delta_{Ph}=7.240$ and $\delta_{C^*H}=5.128$; 80 °C, solution, $\delta_{Ph}=7.265$, $\delta_{C^*H}=5.264$); the latter can be explained by dissociation of Ph–Ph stacked assemblies dissolved in the entrapped solvent and being in equilibrium with the gel network. Thus, the spectroscopic results suggest the existence of **5a** assemblies formed by Ph–Ph interactions both at pre-gelation concentrations and in the solution entrapped by the gel network. Due to similar gelation properties, we assume that for **1a** the favourable lipophilic interactions and hydrophobic effects[22] between isobutyl groups could stabilise a similar type of association in water (Figure 12). The FTIR data for **1a** and **5a** xerogels (prepared from water/DMSO gels; Table 3) show that the intermolecular hydrogen bonding between oxalyl amide and carboxylic groups also stabilises the assembly of gel fibres. It is well known that intermolecular hydrogen bonding is highly disfavoured in water due to strong competitive solvent effects. However, hydrogen bonds can form in water if sufficiently large primary associates are formed enabling formation of many hydrogen bonds possibly in the co-operative manner. Consequently, the gelation of water by **1a** and **5a** can be rationalised by the initial formation of elongated primary assemblies driven by intermolecular lipophilic and $\pi-\pi$ stacking interactions. Such assemblies may further organise into fibers or fiber bundles by lateral hydrogen bonding involving both the oxalyl amide and carboxyl groups (Figure 12).

It is important to note that the same types of spectroscopically identified intermolecular interactions that stabilize fibres of **5a**-hydrogel can be also found in the crystal structure of non-gelling (±)-**5a** (Figure 11). The intermolecular, in plane hydrogen bonding between oxalyl amide units forms α network along *a* axis and the bilayer formed by Ph–Ph interactions and carboxylic hydrogen bonding represents the organisation along the *b* axis. However, the presence of both enantiomers allows formation of the centrosymmetric dimers and the organisation along *c* axis favourable for crystallisation. The latter organisation is not possible for single enantiomer of **5a** which forms gel instead crystallisation in the same solvent system. It should be noted that the organisation along the *b* axis in the crystals of (±)-**5a** closely resembles that in gel fibres of (*R*,*R*)-**5a** postulated on the basis of spectroscopic results (Figure 12).

Formation of the primary assemblies in water requires *cis*-arrangement of substituents on asymmetric carbons of the oxalyl amide gelators. Molecular modelling generated the low energy conformations of **5a** and **1a** (Figure 13) with *cis*-arrangement of Ph and isobutyl groups, respectively; the same arrangement is found in the molecular structure of each enantiomer of *rac*-**5a** (Figure 9 and 11). The substituents form sufficiently deep and wide pockets for intermolecular lip-

0947-6539/01/0715-3336 $ 17.50+.50/0 *Chem. Eur. J.* **2001**, *7*, No. 15

ophilic (Ph–Ph and *i*Bu–*i*Bu) interactions shown schematically in Figure 12. For the non-gelling **2a**, **3a**, **4a** and *meso*-**5**, the low energy conformations with shallow or partly occupied pockets (Figure 13) were generated; and for the non-gelling *meso*-**5** and **4a** further conformations with a *trans*-arrangement of the substituents were generated. The latter conformations are less favourable for intermolecular lipophilic interactions compared with those of **1a** and **5a**; a fact which explains the lack of water gelation ability of **2a**, **3a**, **4a** and *meso*-**5**.

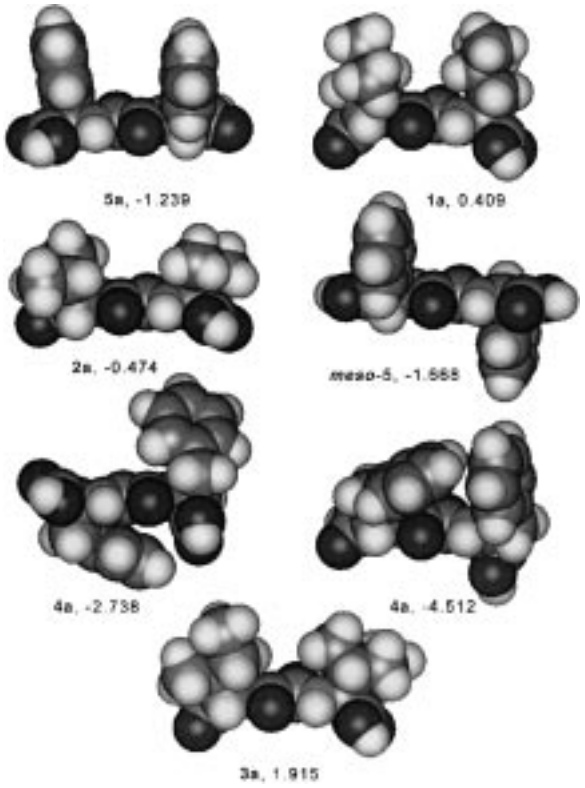

Figure 13. CPK presentation of low energy conformations and TRIPOS force field energies of selected gelators and non-gelling derivatives generated by systematic conformational search using SYBYL molecular modelling software of TRIPOS Inc.

Gelation of organic solvents: Contrary to highly polar water, water/DMSO and water/DMF systems, **1a**, **2a** and **3a** showed similar gelation of lipophilic solvent mixtures (Table 1). This implies that in lipophilic media the intermolecular hydrogen bonding, but not lipophilic interactions, dominates the organisation which leads to formation of gel network. The FTIR data (Table 3) for the gels with lipophilic solvents are in accord with this conclusion. The temperature dependent FTIR of **2a**/$CH_3CN/CHCl_3$ gel (Figure 4) as well as temperature and concentration dependent ^{1}H NMR spectra of the same gel with deuterated solvents (Figure 7) reveal involvement of oxalyl amide and carboxylic groups in intermolecular hydrogen bonding. Figure 7a shows slight upfield shifts of oxalyl amide NH protons upon temperature increase of the gel sample; the effect should correspond to dissociation of small **2a** assemblies dissolved in the entrapped solution. Also, the very slight downfield shifts of **2a**-C*H, -methine and -methyl protons (Figure 7b–d) by temperature increase indicate their mutual shielding in the same assemblies. In the concentration dependent spectra (Figure 7e) the NH protons are shifted downfield until the critical gelation concentration of 0.074 mol dm^{-3} is reached. Thus, at the pre-gelation concentrations the assemblies are formed also by intermolecular hydrogen bonding between oxalyl amide fragments.

The crystal structure of **2a** (Figure 10) determined from the crystals directly grown from the EtOAc/petroleum ether gel shows the existence of intermolecular hydrogen bonding between oxalyl amide units and carboxylic groups in accord with FTIR and ^{1}H NMR observations. In the *a*,*b* plane the **2a** dimers formed by out-of-plane hydrogen bonds between oxalyl amide fragments are connected with other dimers through COOH$\cdots$O=C-NH hydrogen bonding (Figure 10c). The organisation along *c* axis is double helical and presents the only fibre-like organisation which might be related to that in gel fibres. Menger[8d] observed double helical organisation in the crystal structure of dibenzoyl-L-cystine gelator; the organisation was taken to correspond to that in gel fibres. In our case, the temperature dependent ^{1}H NMR shifts of **2a** protons in the gel suggest the presence of small dissolved **2a** assemblies in equilibrium with the gel network; hence the organisation in the assemblies should resemble that in gel fibres. Since the crystallisation starts within the gel, the crystallisation centres should form in the entrapped solution involving dissolved assemblies. Consequently, the double helical organisation found in direction of the *c* axis may resemble that in gel fibres. At present, however, there is no direct experimental evidence for such a conclusion. The fact that identical intermolecular interactions were found in the crystal structure and in the gel fibres and that observed double helical organisation is favourable for the lipophilic EtOAc/petroleum ether solvent system (possessing most of the polar groups in the core and *i*Pr groups at the periphery of the double helix) may be taken as supportive for the above conslusion.

Linear T_g/ε correlation for 1a/lower *n*-alcohol gels: The linear T_g/ε correlation revealed for **1a**/C_1-C_6 alcohol gels (Figure 1) implies that alcohol solvating power has the major influence on the thermal stability of the gel. Hence, better solubility and less efficient gel network assembly of **1a** in the alcohols of higher dielectric contant can be expected. The opposite holds for alcohols of lower ε values where more efficient assembly and hence the gels with higher T_g values are formed. In accord with this, for **1a**/[D_6]EtOH gel the low ΔH_{gel} of -14 kJ mol^{-1} was determined (Table 4); at room temperature only 38% of **1a** molecules are assembled in the gel network and 62% are dissolved in the entrapped ethanol. The results for **2a** gel with much less polar $CD_3CN/CDCl_3$ solvent mixture, reflect the influence of solvent polarity on thermal stability of the gel and give the ΔH_{gel} of -29 kJ mol^{-1}.

In contrast to **1a**/(C_1-C_6) alcohol gels, the gels with higher ($C_7-C_{10,}$ and C_{12}) alcohols and those with *i*BuOH and 2-methyl-2-butanol dissobey the T_g/ε correlation exhibiting much lower T_g values than expected from their ε values. The comparison of isobutanol ($\varepsilon = 17.93$; $T_g = 53\,^\circ$C) and 1-butanol

($\varepsilon = 17.84$; $T_g = 97\,^{\circ}C$) gels appears very instructive. Despite the close dielectric constants the isobutanol gel showed a lower T_g by 44 °C than the 1-butanol gel (Table 2). It is likely that the dispersive interactions between **1a** and *i*BuOH and long and foldable alkyl chains of higher *n*-alcohols enhance its solubility in these solvents.[23, 24] Estimation of the maximal pre-gelation concentrations of **1a** in 1-BuOH (0.003 mg mL^{-1}), *i*BuOH (0.008 mg mL^{-1}), *n*-heptanol and *n*-octanol (0.003 mg mL^{-1}) support this conclusion. The pre-gelation concentrations of **1a** in *i*BuOH is more than twice of that in 1-BuOH despite the very close ε values of the two alcohols; for *n*-heptanol ($\varepsilon = 11.75$) and *n*-octanol ($\varepsilon = 10.3$) the pre-gelation concentrations are comparable to 1-BuOH with a much higher dielectric constant of $\varepsilon = 17.84$.

Water versus organic solvent gelation: Gelators **1a** and **5a** exhibited ambidextrous gelation of highly polar water, water/DMSO and water/DMF mixtures and of much less polar organic solvents (Table 1). Described spectroscopic investigations show that the ambidextrous gelation is the result of different organisation in two media; in water it is governed mostly by lipophilic interactions and in organic solvents by intermolecular hydrogen bonding. For **1a**/[D$_6$]EtOH gel the ΔH_{gel} of -14 kJ mol^{-1} was determined together with only 38% network assembled and 62% dissolved **1a** molecules in the gel at 20 °C; however, for **1a**/water/[D$_6$]DMSO (3.3:1) gel with much more polar solvent system the ΔH_{gel} of -36 kJ mol^{-1} and 80% of assembled **1a** molecules was determined (Table 4). The latter solvent system is much less favourable for intermolecular hydrogen bonding between gelator molecules. Thus, the fact that water/[D$_6$]DMSO gel is more stable for 22 kJ mol^{-1} and that the assembly–dissolution equilibrium lies much more on the assembly side despite the lower total concentration of **1a** clearly points toward lipophilic interactions and hydrophobic effects as the main stabilising forces in this gel assembly.

Conclusion

Enantiomerically pure bis(amino acid) oxalyl amides **1a** and **5a** exhibit ambidextrous gelling properties of water, water containing solvent mixtures and lipophilic organic solvent systems giving stable and thermoreversible gels. Their racemates and *meso*-diastereoisomers lack gelation ability. The intermolecular lipophilic interactions between substituents on asymmetric carbons and lateral hydrogen bonding were found to stabilise network assemblies of aqueous gels. However, in organic solvent gels, intermolecular hydrogen bonding involving oxalyl amide fragments and carboxylic groups represents the dominant intermolecular interactions that stabilise these gel networks. It was found that the ^{1}H NMR spectroscopy of gels detects the gelator molecules or assemblies present in the entrapped solvent. The concentration of dissolved gelator molecules increase by rising sample temperature due to dissociation of a gel network. The same temperature dependent network assembly–dissolution equilibrium is observed by FTIR. Both methods were used for determination of K_{gel} and ΔH_{gel} and give the latter values in excellent agreement. For **1a** gels with C_1–C_6 alcohols, the linear T_g/alcohol dielectric constant correlation was found showing the dominant influence of alcohol polarity on the thermal stability of a gel. The characteristic intermolecular interaction patterns existing in gel fibres of aqueous (**1a**, **5a**) and organic solvent (**2a**) gels identified by spectroscopic investigations (^{1}H NMR, FTIR, UV, fluorescence) were also found in the crystal structures of **2a** and (±)-**5a.** The double helical organisation found in the **2a** crystals grown from EtOAc/petroleum ether gel may resemble organisation in gel fibres. Ageing of unstable **2a**/organic solvent gels leads to formation of various crystalline shapes such as crystalline tubes, spheres, fibres, macrocycles and catenanes of micrometer dimensions. This could be the consequence of crystallisation occurring in the presence of gel network. The formation of various crystalline forms by crystallisation of inorganic materials within gels is described in the very recent review.[25]

Experimental Section

General: Melting points were determined on Kofler stage and are uncorrected. ^{1}H and ^{13}C NMR spectra were recorded at 300 MHz and 75 MHz, respectively, on a Gemini 300 spectrometer (TMS was used as internal standard). FTIR spectra were recorded on a Perkin–Elmer PE 2000. UV/VIS measurements were carried out on a Cary 5 and PU 8730 UV/VIS spectrophotometer. Optical rotations were measured on an optical activity AA-10 automatic polarimetar using the wavelength of 589.3 nm. TLC was performed on silica gel coated Merck 60 F_{254} silica plates and column chromatography using 230–240 mesh Merck 60 silica gel. All chemicals were of the best grade commercially available and were used without purification. Solvents were purified according to standard procedures; dry solvents were obtained according to literature methods and stored over molecular sieves. The following compounds were previously described in the literature: **4a**,[26] **4b**,[28] **5a**,[27] **1b**,[29] **2b**[30] and **2a**,[30] however, the latter was not fully characterised.

General procedure for preparation of bis(amino acid) oxalyl amides 1a–6a: A solution of oxalyl chloride (4.95 mmol) in CH_2Cl_2 (5 mL) and 4 M aqueous KOH (2.1 mL) were simultaneously added dropwise within 40 min to a cooled (−10 °C) solution of the corresponding (*R*)- or (*S*)-amino acid (6.6 mmol) in 2 M KOH (5 mL). The stirring was continued for 30 min at 0 °C and for another 30 min at room temperature. Organic layer was separated, and the aqueous layer diluted with H_2O (10 mL) and acidified with 10%-formic acid (pH 2.5). The solid or gelatinous precipitate formed was crashed in ultra-sound bath, left to stand at 4 °C for 2 h, filtered, washed with water and dried under reduced pressure.

***N,N'*-Oxalyl-bis(LeuOH) (1a)**: Yield: 85.7%; m.p. 215–216 °C; $[\alpha]_D^{20} = -13$ ($c = 1$ in DMSO); ^{1}H NMR (300 MHz, [D$_6$]DMSO, 20 °C): $\delta = 8.60$ (d, ^3J(H,H) = 8.4 Hz, 2H; NH), 4.20 (dt, ^3J(H,H) = 3.0, 8.9 Hz, 2H; C*H$_\alpha$), 1.75–1.54 (m, 6H; CH$_\gamma$, CH$_{2\beta}$), 0.86/0.88 (2d, ^3J(H,H) = 5.1 Hz, 6H each; CH$_3$); ^{13}C NMR (75.5 MHz, [D$_6$]DMSO), 20 °C): $\delta = 173.5$ (COOH), 159.7 (CONH), 51.4 (C*H$_\alpha$), 40.2 (CH$_{2\beta}$), 24.5 (CHγ), 23.1/21.5 (CH$_3$); IR (KBr): $\tilde{\nu} = 3300$ (NH), 1730 (COOH), 1660 (amide I), 1520 (amide II) cm^{-1}; elemental analysis calcd (%) for $C_{14}H_{24}N_2O_6 \cdot H_2O$ (334.364): C 50.29, H 7.84, N 8.38; found C 50.54, H 8.03, N 8.58.

***N,N'*-Oxalyl-bis(ValOH) (2a)**: Yield: 62.9%; m.p. 124–125 °C; $[\alpha]_D^{20} = +16$ ($c = 1$ in MeOH); ^{1}H NMR (300 MHz, CD$_3$OD, 20 °C): $\delta = 8.55$ (d, ^3J(H,H) = 8.6 Hz, traces; NH), 4.46 (d, ^3J(H,H) = 5.1 Hz, 2H; C*H$_\alpha$), 2.42–2.29 (m, 2H; CH$_\beta$), 1.08/1.07 (2d, ^3J(H,H) = 6.8 Hz, each 6H; CH$_3$); ^{13}C NMR (75.5 MHz, CD$_3$OD, 20 °C): $\delta = 174.1$ (COOH) 161.5 (CONH), 59.5 (C*H$_\alpha$), 32.2 (CH$_\beta$), 19.6/18.4 (CH$_3$); IR (KBr): $\tilde{\nu} = 3290/3130$ br (NH), 1728 (COOH), 1660 (amide I), 1525 (amide II) cm^{-1}; elemental analysis calcd (%) for $C_{12}H_{20}N_2O_6$ (288.296): C 49.99, H 6.99, N 9.72; found C 50.07, H 7.20, N 9.84.

0947-6539/01/0715-3338 $ 17.50+.50/0 *Chem. Eur. J.* **2001**, *7*, No. 15

***N,N′*-Oxalyl-bis(IleOH) (3a)**: Yield: 42.6%; m.p. 139–142°C (xerogel from MeOH/diethyl ether); $[\alpha]_D^{20} = +40$ ($c = 0.5$ in MeOH); ^{1}H NMR (300 MHz, [D$_6$]DMSO, 20°C): $\delta = 8.33$ (d, ^3J(H,H) = 8.2 Hz, 2H; NH), 4.09 (dt, ^3J(H,H) = 5.7, 8.2 Hz, 2H; C*H$_\alpha$), 1.97–1.84 (m, 2H; CH$_\beta$), 1.51–1.30/1.22–1.08 (2m, 2H each; CH$_{2\gamma}$), 0.88–0.84 (m, 12H; CH$_{3\gamma}$, CH$_{3\delta}$); ^{13}C NMR (75.5 MHz, CD$_3$OD, 20°C): $\delta = 175.2$ (COOH), 161.4 (CONH), 59.3 (C*H$_\alpha$), 38.9 (CH$_\beta$), 26.4 (CH$_{2\gamma}$), 16.3 (CH$_{3\gamma}$), 12.1 (CH$_{3\delta}$); IR (KBr): $\tilde{\nu} = 3310$ (NH), 1727 (COOH), 1659/1652 (amide I), 1512 (amide II) cm^{-1}; elemental analysis calcd (%) for C$_{14}$H$_{24}$N$_2$0$_6$·H$_2$O (334.364): C 50.29, H 7.84, N 8.38; found C 50.30, H 7.92, N 8.39.

***N,N′*-Oxalyl-bis(TrpOH) (6a)**: Yield: 66.9%; m.p. 224–227°C; $[\alpha]_D^{20} = +95$ ($c = 1$ in DMSO); ^{1}H NMR (300 MHz, [D$_6$]DMSO, 20°C): $\delta = 10.85$ (s, 2H; indol-NH), 8.44 (d, ^3J(H,H) = 7.75 Hz, 2H; CONH), 7.48/7.33 (2d, ^3J(H,H) = 7.4 Hz, 2H each; C4′H, C7′H), 7.07 (s, 2H; C2′H), 7.04/6.90 (2t, ^3J(H,H) = 7.4 Hz, 2H each; C5′H, C6′H), 4.40 (dt, ^3J(H,H) = 5.8, 7.8 Hz, 2H; C*H$_\alpha$), 3.24 (d, ^3J(H,H) = 5.8 Hz, 4H; CH$_{2\beta}$); ^{13}C NMR (75.5 MHz, [D$_6$]DMSO), 20°C): $\delta = 173.0$ (COOH), 159.3 (CONH), 136.3, 127.9, 123.8, 121.0, 118.6, 118.5, 111.5/110.2 (C$_{arom}$), 54.2 (C*H$_\alpha$), 26.8 (CH$_{2\beta}$); IR (KBr): $\tilde{\nu} = 3408/3300$ (NH), 1660/1600 (br) (amide I), 1515 (amide II) cm^{-1}; elemental analysis calcd (%) for C$_{24}$H$_{22}$N$_4$0$_6$·2H$_2$O (498.48): C 57.82, H 5.26, N 11.24; found C 58.07, H 5.18, N 11.14.

***N,N′*-Oxalyl-bis(isoleucine methyl ester) (3b)**: A solution of oxalyl chloride (0.185 mL, 2.12 mmol) was added to a cooled (0°C) solution of H-Ile-OMe·HCl (0.802 g 4.41 mmol) and TEA (1.23 mL, 8.82 mmol) in dry CH$_2$Cl$_2$ (15 mL), and the reaction mixture was stirred at 0°C for 30 min and overnight at room temperature. Dichloromethane (10 mL) was added and the mixture washed with water, aq. AcOH and 5% NaHCO$_3$. Organic layer was separated, dried (Na$_2$SO$_4$) and the solvent evaporated. Recrystallisation (CH$_2$Cl$_2$/light petroleum) give the title compound (0.596 g, 81.6%). M.p. 99–101°C (from CH$_2$Cl$_2$/diethyl ether); $[\alpha]_D^{20} = -12$ ($c = 0.5$ in MeOH); ^{1}H NMR (300 MHz, CDCl$_3$, 20°C, TMS): $\delta = 8.98$ (d, ^3J(H,H) = 9.0 Hz, 2H; NH), 4.46 (dd, ^3J(H,H) = 5.1, 9.0 Hz, 2H; C*H$_\alpha$),3.68 (s, 6H, OCH$_3$), 1.96–1.83 (m, 2H; CH$_\beta$), 1.44–1.33 (2m, 2H each; CH$_{2\gamma}$), 1.25–1.08/0.87–0.83 (m, 12H; CH$_{3\gamma}$, CH$_3$); ^{13}C NMR (75.5 MHz, CDCl$_3$, 20°C): $\delta = 170.9$ (COOMe), 159.0 (CONH), 56.7 (CH$_\alpha$), 52.0 (OCH$_3$), 37.6 (CH$_\beta$), 24.7 (CH$_{2\gamma}$), 15.1 (CH$_{3\gamma}$), 11.1 (CH$_3$); IR (KBr): $\tilde{\nu} = 3285$ (NH), 1753 (COOMe), 1663 (amide I), 1533 (amide II) cm^{-1}; elemental analysis calcd (%) for C$_{16}$H$_{28}$N$_2$O$_6$ (344.40): C 55.80, H 8.20, N 8.13; found C 55.86, H 8.37, N 8.26.

***N,N′*-Oxalyl-bis[(*R*)-phenylglycine methyl ester)] (5b)**: Following the procedure described for preparation of **3b**, (*R*)-H-Phg-OMe·HCl (0.414 g, 2.05 mmol) and oxalyl chloride (0.85 mL, 0.97 mmol) gave **5b** (0.288 g, 76.7%). M.p. 183–184°C (from CH$_2$Cl$_2$/light petroleum ether), $[\alpha]_D^{20} = +236$ ($c = 0.5$ in CH$_2$Cl$_2$); ^{1}H NMR (300 MHz, CDCl$_3$, 20°C, TMS): $\delta = 8.24$ (d, ^3J(H,H) = 7.3 Hz, 2H; NH), 7.35 (s, 10H; H$_{arom}$), 5.51 (d, ^3J(H,H) = 7.5 Hz, 2H; C*H$_\alpha$), 3.75 (s, 6H; OCH$_3$); ^{13}C NMR (75.5 MHz, CDCl$_3$, 20°C): $\delta = 169.8$ (COOMe), 158.3 (CONH), 136.2, 128.9, 128.7/127.2 (C$_{arom}$), 56.5 (CH$_\alpha$), 52.8 (OCH$_3$); IR (KBr): $\tilde{\nu} = 3275$ (NH), 1742 (COOMe), 1654 (amide I), 1500 (amide II) cm^{-1}; elemental analysis calcd (%) for C$_{20}$H$_{20}$N$_2$O$_6$ (384.382): C 62.49, H 5.24, N 7.29; found C 62.20 H 5.51, N 7.51.

***N,N′*-Oxalyl-bis(leucylamide) (1c)**: A solution of **1b** (0.250 g, 0.73 mmol) in conc. NH$_3$/MeOH (25 mL) was kept for 7 d at 4°C. The precipitate was filtered off washed with MeOH and dried under reduced pressure. Yield: 0.163 g, 64.1%; m.p. 273–276°C (from DMSO/EtOAc); $[\alpha]_D^{20} = -2$ ($c = 1$ in DMSO); ^{1}H NMR (300 MHz, [D$_6$]DMSO, 20°C): $\delta = 8.47$ (d, ^3J(H,H) = 8.8 Hz, 2H; NH), 7.49/7.14 (2s, 2H each; CONH$_2$), 4.29 (dt, ^3J(H,H) = 3.8, 8.8 Hz, 2H; C*H$_\alpha$), 1.70–1.48 (m, 6H; CH$_{2\beta}$, CH$_\gamma$), 0.89/0.88 (2d, ^3J(H,H) = 5.4 Hz, 6H each; CH$_3$); ^{13}C NMR (75.5 MHz, [D$_6$]DMSO), 20°C): $\delta = 173.4$ (CONH$_2$), 159.6 (CONH), 51.6 (CH$_\alpha$), 40.9 (CH$_{2\beta}$), 24.5 (CH$_\gamma$), 23.0/21.6 (CH$_3$); IR (KBr): $\tilde{\nu} = 3400$, 3280/3210 (NH), 1660 br (amide I), 1512 (amide II) cm^{-1}; elemental analysis calcd (%) for C$_{14}$H$_{26}$N$_4$O$_4$·2H$_2$O (350.412): C 47.98, H 8.63, N 15.99; found C 47.99, H 8.57, N 15.79.

***N,N′*-Oxalyl-bis(valylamide) (2c)**: A solution of **2b** (0.050 g, 0.16 mmol) in CH$_2$Cl$_2$ (1 mL) and conc. NH$_3$/MeOH (10 mL) was kept for 8 d at room temperature. The precipitate was filtered off, washed with MeOH and dried under reduced pressure. Yield: 0.043 g, 95.0%; m.p. > 330°C (from DMF/CH$_2$Cl$_2$); $[\alpha]_D^{20} = +37$ ($c = 0.5$ in DMSO); ^{1}H NMR (300 MHz, [D$_6$]DMSO, 20°C): $\delta = 8.18$ (d, ^3J(H,H) = 9.3 Hz, 2H; NH), 7.61/7.26 (2s, 2H each; CONH$_2$), 4.12 (dd, ^3J(H,H) = 6.7, 9.3 Hz, 2H; CH$_\alpha$), 2.06 (sext, ^3J(H,H) = 7 Hz, 2H; CH$_\beta$), 0.88/0.83 (2d, ^3J(H,H) = 6.7 Hz, 6H each; CH$_{3\gamma}$); ^{13}C NMR (75.5 MHz, [D$_6$]DMSO), 20°C): $\delta = 172.1$ (CONH$_2$), 159.4 (CONH), 58.2 (CH$_\alpha$), 30.8 (CH$_\beta$), 19.3/17.9 (CH$_{3\gamma}$); IR (KBr): $\tilde{\nu} = 3410$, 3280/3210 (NH), 1660/1647 (amide I), 1516 (amide II) cm^{-1}; elemental analysis calcd (%) for C$_{12}$H$_{22}$N$_4$O$_4$ (286.328): C 50.33, H 7.74, N 19.57; found C 50.28, H 7.62, N 19.47.

***N,N′*-Oxalyl-bis(isoleucylamide) (3c)**: A solution of **3b** (0.323 g, 0.94 mmol) in conc. NH$_3$/MeOH (30 mL) was kept for 7 d at room temperature. The precipitate was filtered off washed with MeOH and dried under reduced pressure. The product partly racemised. Yield: 0.225 g, 77.7%; m.p. 304–305°C (from DMSO); $[\alpha]_D^{20} = +12$ ($c = 0.5$ in DMSO); ^{1}H NMR (300 MHz, [D$_6$]DMSO, 20°C): $\delta = 8.21$ (d, ^3J(H,H) = 9.2 Hz, 2H; NH), 7.59/7.24 (2s, 2H each; CONH$_2$), 4.14 (dt, ^3J(H,H) = 7.3, 9.2 Hz, 2H; CH$_\alpha$), 1.86–1.77/1.47–1.36/1.10–0.96 (3m, 2H each; CH$_\beta$, CH$_{2\gamma}$), 0.87–0.82 (m, 12H; CH$_{3\gamma}$, CH$_3$); ^{13}C NMR (75.5 MHz, [D$_6$]DMSO), 20°C): $\delta = 171.8$ (CONH$_2$), 159.1 (CONH), 57.3 (CH$_\alpha$), 36.8 (CH$_\beta$), 24.2 (CH$_{2\gamma}$), 15.2 (CH$_{3\gamma}$), 10.7 (CH$_3$); IR (KBr): $\tilde{\nu} = 3410$, 3278/3210 (NH), 1680, 1660, 1653/1645 (amide I), 1516 (amide II) cm^{-1}; elemental analysis calcd (%) for C$_{14}$H$_{26}$N$_4$O$_4$ (314.38): C 53.48, H 8.34, N 17.82; found C 53.42, H 8.47, N 17.72.

***N,N′*-Oxalyl-bis(phenylalanylamide) (4c)**: A solution of **4b** (0.346 g, 0.84 mmol) in conc. NH$_3$/MeOH (35 mL) was kept 7 d at 4°C. The precipitate was filtered off washed with MeOH and dried under reduced pressure. Yield: 0.272 g, 84.8%; m.p. 287–288°C (from DMF); $[\alpha]_D^{20} = -13$ ($c = 0.5$ in DMSO); ^{1}H NMR (300 MHz, [D$_6$]DMSO, 20°C): $\delta = 8.24$ (d, ^3J(H,H) = 8.2 Hz, 2H; NH), 7.46/7.09 (2brs, 2H each; CONH$_2$), 7.22/7.17 (2brs, 10H; CH$_{arom}$), 4.49 (brs, 2H; C*H$_\alpha$), 3.14–2.96 (m, 4H; CH$_{2\beta}$); ^{13}C NMR (75.5 MHz, [D$_6$]DMSO), 20°C): $\delta = 171.8$ (CONH$_2$), 159.0 (CONH), 137.3, 129.1, 128.1/126.4 (C$_{arom}$), 53.9 (CH$_\alpha$), 37.1 (CH$_{2\beta}$); IR (KBr): $\tilde{\nu} = 3454$, 3382, 3284/3200 (NH), 1659 (amide I), 1506 (amide II) cm^{-1}; elemental analysis calcd (%) for C$_{20}$H$_{22}$N$_4$O$_4$ (382.408): C 62.81, H 5.80, N 14.65; found C 63.06, H 5.99, N 14.57.

(±)-[*N,N′*-Oxalyl-bis(phenylglycylamide)] (5c): A solution of **5b** (0.370 g, 0.96 mmol) in DMF (5 mL) and conc. NH$_3$/MeOH (35 mL) was kept 14 d at room temperature. The precipitate was filtered off, washed with MeOH and dried under reduced pressure. Yield: 0.240 g, 70.4%; m.p. 301–303°C (from DMF/CH$_2$Cl$_2$); The product completely racemised, $[\alpha]_D^{20} = 0$ ($c = 0.5$ in DMSO); ^{1}H NMR (300 MHz, [D$_6$]DMSO, 20°C): $\delta = 8.64$ (d, ^3J(H,H) = 7.6 Hz, 2H; NH), 7.81/7.34 (2s, 2H each; CONH$_2$), 7.43–7.29 (m, 10H; CH$_{arom}$), 5.35 (s, 2H; C*H$_\alpha$); ^{13}C NMR (75.5 MHz, [D$_6$]DMSO), 20°C): $\delta = 170.8$ (CONH$_2$), 158.7 (CONH), 138.3, 128.8, 128.2/127.2 (C$_{arom}$), 56.2 (C*H$_\alpha$); IR (KBr): $\tilde{\nu} = 3370$, 3268/3188 (NH), 1657 (amide I), 1496 (amide II) cm^{-1}; elemental analysis calcd (%) for C$_{18}$H$_{18}$N$_4$O$_4$ (354.356): C 61.01, H 5.12, N 15.81; found C 60.85, H 5.27, N 15.74.

Gelation experiments: The experiments were performed by dissolution of the weighted amount of a compound (10 mg) in a measured volume of selected pure solvent or solubilising component. In the first case heating of the sample is needed to produce dissolution. Cooling to room temperature produced gels as shown in Table 1. In the second procedure, a measured volume of a second solvent of lower polarity was added until the gel was formed. The procedure being reminiscent of two-solvents recrystallisation is repeated until formation of a loose gel or dissolution is observed.

Estimation of maximal pre-gelation concentration of 1a: To 5 mg of **1a** (exactly weighted), *n*BuOH, *i*BuOH, *n*-heptanol or *n*-octanol was added in 2 μL volume portions, the suspension heated to boiling and cooled. The procedure was repeated until the solution of low viscosity instead a gel was formed at room temperature.

TEM and SEM investigations: Transmision electron micrographs were negatively stained by osmic acid. JOEL JSM-5800 scanning electron microscope was used for taking SEM pictures.The frozen gel specimen (liquid nitrogen) was evaporated by a vacum pump for 5–24 h. The dry sample was shielded by gold (10 Å). The accelerating voltage of SEM was 20 kV.

Molecular modelling: Molecular modelling was performed using the SYBYL Version 6.3 software of TRIPOS INC. The molecules were constructed using Builder package and fully minimised. The systematic conformational search using TRIPOS force field was done by 30° increment rotations around six bonds (C*-R, R = alkyl or aryl; C*-NH and C*-

COOH). The lowest energy conformations were selected and fully minimised.

Crystal structure determination of 2a and (±)-5a: For crystallizaton of **2a**, a small beaker containing ethyl acetate solution (60 mg mL^{-1}) was immmersed into a bottle with petroleum ether (40–70 °C) serving as a reservoir. Slow vapour diffusion of petroleum ether into the solution induced a gel formation. Over the period of a few days at room temperature prismatic crystals were grown within a gel. The crystals of **5a** were obtained from DMF solution (20mg mL^{-1}) using vapour diffusion from water reservoir at room temperature, over a few days. Data collection of (±)-**5a** was at 100 K whereas for **2a** was at room temperature. The crystallographic data and details of data collection and refinement have been listed in Table 8.[31–34] The absorption corrections on intensities of **2a** and (±)-**5a** were applied using analytical method [Meulenaer-Tompa] incorporated into PLATON.[34] L-amino acids were used in synthesis of the compounds studied and during structure determination chirality was assigned accordingly. Scattering factors used in the calculations were from SHELX97.[33] Hydrogen atom positions were calculated on stereochemical grounds and refined using the SHELX97 riding model. The exceptions were hydrogen atoms involved in hydrogen bonding; they were located from the difference Fourier syntheses and refined. The crystal structure of (±)-**5a** includes the solvent molecules. The thermal gravimetric analysis revealed 2.75 water molecules per one formula unit of **5a**. The amount of solvent molecules determined experimentally matches the number of electrons calculated by SQUEEZE option in the program PLATON.[34] The final R factors and the values of residual electron densities, $\Delta\rho$ (Table 7) are given after the applied squeeze option for the structure (±)-**5a**. The molecular structures were illustrated by the ORTEPH.[35]

Crystallographic data (excluding structure factors) for the structures reported in this paper have been deposited with the Cambridge Crystallographic Data Centre as supplementary publication no. CCDC-146381 (**2a**) and -146383 [(±)-**5a**]. Copies of the data can be obtained free of charge on application to CCDC, 12 Union Road, Cambridge CB2 1EZ, UK (fax: (+44) 1223-336-033; e-mail: deposit@ccdc.cam.ac.uk).

Table 8. Crystallographic data, structure solution and refinement of **2a** and (±)-**5a**.

	2a	(±)-**5a**
formula	$C_{12}H_{20}N_2O_6$	$C_{18}H_{16}N_2O_6 \cdot 2.75\,H_2O$
M_r	288.30	405.87
crystal system	orthorhombic	triclinic
space group	$P2_12_12$ (No. 18)	$P\bar{1}$ (No. 2)
a [Å]	12.4291(7)	5.0971(4)
b [Å]	18.1252(6)	13.6399(6)
c [Å]	6.6381(3)	14.7236(5)
α[°]		74.670(3)
β [°]		81.905(5)
γ [°]		79.631(3)
V [Å^3]	1495.4(1)	966.39(9)
Z	4	2
ρ [g cm^{-3}]	1.281	1.395
radiation	$Mo_{K\alpha}$	$Cu_{K\alpha}$
λ [Å]	0.71069	1.54184
Θ range [°]		
for cell determination	8.4–21.5	40.4–46.8
μ [mm^{-1}]	0.1	0.96
T [K]	295(3)	100(3)
crystal form	prism	plate
crystal size [mm]	0.19 × 0.26 × 0.28	0.14 × 0.11 × 0.04
crystal colour	colourless	colourless
diffractometer	Enraf-Nonius CAD4	Enraf-Nonius CAD4
data collection method	$\omega/2\theta$	$\omega/2\theta$
absorption correction	analytical	analytical
total data collected	1836	4446
unique data	778	3936
observed data		
$[I > 2\sigma(I)]$	145	2198
R_{int}	0.000	0.0298
Θ_{max} [°]	26.31	74.33
range of h, k, l	−15 → 0	−6 → 0
	−22 → 0	−17 → 16
	−8 → 0	−18 → 18
standard reflections	3	3
intensity dacay [%]	3	0
refinement on	F^2	F^2
R_1 [$F_o > 4\sigma(F_o)$]	0.0375	0.0478
$wR_2(F^2)$, all data	0.1079	0.1276
S	1.106	0.981
parameters	201	268
largest difference peak, hole [e Å^{-3}]	0.28, −0.20	0.35, −0.29
data reduction program	HELENA	HELENA
structure solution program	SIR97	SIR97
structure refinement program	SHELXL97	SHELXL97
preparation of material for publication (program)	PLATON	PLATON

Acknowledgements

The financial support from Croatian Ministry of Science and Technology and COST D-11 Supramolecular Chemistry project D11/0015/99 are gratefully acknowledged. The authors thank Dr. N. Ljubešić, Rudjer Bošković Institute, for TEM and Dr. M. Tudja, PLIVA, for SEM experiments.

[1] J.-M. Lehn, *Supramolecular Chemistry. Concepts and perspectives*, VCH, Weinheim, **1995**.

[2] a) D. Venkataraman, S. Lee, J. Zhang, J. S. Moore, *Nature* **1994**, *371*, 591–593; b) G. R. Desiraju, *Crystal Engineering. The Design of Organic Solids*, Elsevier, Amsterdam, **1989**.

[3] J.-H.Furhop, *Membranes and Molecular Assemblies*: *the Synkinetic Approach*, RSC Monographs in Supramolecular Chemistry (Ed.: J. Fraser Stoddart), **1994**.

[4] Some recent examples on small organic gelators include the following: a) P. Terech, *Ber. Bunsenges. Phys. Chem.* **1998**, *102*, 1630–1643; b) P. Terech, R. G. Weiss, *Chem. Rev.* **1997**, *97*, 3133–3159; c) K. Yoza, N. Amanokura, Y. Ono, T. Akao, H. Shinomori, M. Takeuchi, S. Shinkai, D. N. Reinhoudt, *Chem. Eur. J.* **1999**, *5*, 2722–2729; d) R. Oda, I. Huc, S. J. Candau, *Angew. Chem.* **1998**, *110*, 2853–2858; *Angew. Chem. Int. Ed.* **1998**, *37*, 2689–2691; e) T. Kato, G. Kondo, K. Hanabusa *Chem. Lett.* **1988**, 193–194; f) J. van Esch, S. De Feyter, R. M. Kellog, F. De Schryver, B. L. Feringa, *Chem. Eur. J.* **1997**, *3*, 1238–1243; g) J.-E. S. Sohna, F. Fages, *Chem. Commun.* **1997**, 327–328; h) F. Placin, M. Colomes, J.-P. Desvergne, *Tetrahedron Lett.* **1997**, *38*, 2665–2668.

[5] a) K. Murata, M. Aoki, T. Suzuki, T. Harda, H. Kawabata, T. Komori, F. Ohseto, K. Ukeda, S. Shinkai, *J. Am. Chem. Soc.* **1994**, *116*, 6664–6676, b) R. Mukkamala, R. G. Weiss, *Langmuir* **1996**, *12*, 1474–1482; c) P. Terech, I. Furman, R. G. Weiss, H. Bouas-Laurent, J. P. Desvergne, R. Ramasseul, *Faraday Discuss.* **1995**, *101*, 345–358; d) S. W. Jeong, S. Shinkai, *Nanotechnology* **1997**, *8*, 179–185; e) Y. Hishikawa, K. Sada, R. Watanabe, M. Miyata, K. Hanabusa, *Chem. Lett.* **1998**, 795–796.

[6] a) T. Brotin, R. Utermöhlen, F. Fages, H. Bouas-Laurent, J.-P. Desvergne, *J. Chem. Soc. Chem. Commun.* **1991**, 416–418; b) J. L. Pozzo, G. M. Clavier, M. Colomes, H. Bouas-Laurent, *Tetrahedron* **1997**, *53*, 6377–6390.

[7] P. Terech, V. Rodriguez, J. D. Barnes, G. B. McKenna, *Langmuir* **1994**, *10*, 3406–3418.

[8] a) N. Mizoshita, T. Kutsuna, K. Hanabusa, T. Kato, *J. Chem. Soc. Chem. Commun.* **1999**, 781–782; b) K. Hanabusa, K. Okui, K. Karaki, M. Kimura, H. Shirai, *J. Colloid Interface Sci.* **1997**, *195*, 86–93; c) K. Hanabusa, R. Tanaka, M. Suzuki, M. Kimura, H. Shirai, *Adv. Mater.* **1997**, *9*, 1095–1097; d) F. Menger, Y. Yamasaki, K. K. Catlin, T. Nishimi, *Angew. Chem.* **1995**, *107*, 616–618; *Angew. Chem. Int. Ed. Engl.* **1995**, *34*, 585–586; e) T. T. Stock, N. J. Turner, R. McCague, *J. Chem. Soc. Chem. Commun.* **1995**, 2063–2064; f) E. J. de Vries, R. M. Kellog, *J. Chem. Soc. Chem. Commun.* **1993**, 238–240.

  0947-6539/01/0715-3340 $ 17.50+.50/0

[9] Urea-based gelators: a) see [4f]; b) A. J. Carr, R. Melendez, S. J. Geib, A. D. Hamilton, *Tetrahedron Lett.* **1998**, *39*, 7447–7450; sugar-based gelators: c) see [4c]; d) N. Amanokura, K. Yoza, H. Shinomori, S. Shinkai, D. N. Reinhoudt, *J. Chem. Soc. Perkin Trans. 2* **1998**, 2585–2591; e) K. Inoue, Y. Ono, Y. Kanekiyo, S. Kiyonaka, I. Hamachi, S. Shinkai, *Chem. Lett.* **1999**, 225–226; f) J.-H. Fuhrhop, S. Svenson, C. Boettcher, E. Rössler, H.-M. Vieth, *J. Am. Chem. Soc.* **1990**, *112*, 4307–4312; g) T. Shimizu, M. Masuda, *J. Am. Chem. Soc.* **1997**, *119*, 2812–2818; cyclohexyl amide derivatives: h) see [4e]; arylcyclohexanol derivatives: i) C. M. Garner, P. Terech, J.-J. Allegraud, B. Mistrot, P. Nguyen, A. de Geyer, D. Rivera, *J. Chem. Soc. Faraday Trans.* **1998**, *94*, 2173–2179.

[10] M. Jokić, J. Makarević, M. Žinić, *J. Chem. Soc. Chem. Commun.* **1995**, 1723–1724.

[11] a) J. Dong, Y. Ozaki, K. Nakashima, *Macromolecules* **1997**, *30*, 1111–1117; b) L. Sun, L. J. Kepley, R. M. Crooks, *Langmuir* **1992**, *8*, 2101–2103.

[12] After this work was submitted the ^{1}H NMR study of the cholesterol/stilbene gel appeared (D. C. Duncan, D. G. Whitten *Langmuir* **2000**, *16*, 6445–6452) providing the evidence that the gelator molecules dissolved in the gel liquid and those assembled in the mobile (NMR detectable) gel solid can be detected in the spectrum of a gel in a fast exchange on the NMR time scale. These NMR detectable gelator molecules are in the slow exchange with the solid (NMR undetectable) gel network.

[13] In the several recent publications[5a, 14] the ΔH_{gel} values for the sol to gel transition have been determined from the $\ln[c_{tot}]$ versusu $1/T_g$ plots based on the equation $\ln[c_{tot}] = -\Delta H_{gel}/RT_g + \text{const.}$ derived by Ferry[15] for polymer gels (or by using critical gelation concentration (c_{gc})[8b]in the same equation. As discussed by Shinkai,[5a] in this way obtained δH_{gel} values were considerably higher than those obtained by DSC measurements; in some cases the differences were 30–100 kJ mol^{-1} and the ΔH values appeared independent on the type of a solvent.

[14] G. M. Clavier, J.-F. Brugger, H. Bouas-Laurent, J.-L. Pozzo, *J. Chem. Soc. Perkin Trans. 2* **1998**, 2527–2534.

[15] J. E. Eldridge, J. D. Ferry, *J. Phys. Chem.* **1954**, *58*, 992–996.

[16] IUPAC-IUB Commission on Biochemical Nomenclature, *J. Mol. Biol.* **1970**, *52*, 1–17.

[17] I. L. Karle, D. Ranghanathan, K. Shah, N. K. Vaish, *Int. J. Peptide Protein Res.* **1994**, *43*, 160–165.

[18] I. L. Karle, D. Ranghanathan, *Int. J. Peptide Protein Res.* **1995**, *46*, 18–23.

[19] I. L. Karle, D. Ranghanathan, *Biopolymers* **1995**, *36*, 323–331.

[20] J. Bernstein, R. E. Davies, L. Shimoni, N.-L. Chang, *Angew. Chem.* **1995**, *107*, 1689–1708; *Angew. Chem. Int. Ed. Engl.* **1995**, *34*, 1555–1573.

[21] S. Coe, J. J. Kane, T. L. Nguyen, L. M. Toledo, E. Winiger, F. W. Fowler, J. W. Lauher, *J. Am. Chem. Soc.* **1997**, *119*, 86–93.

[22] H.-J. Schneider, A. Yatsimirsky, *Principles and Methods in Supramolecular Chemistry*, Wiley, Chichester, **2000**; H.-J. Schneider, *Angew. Chem.* **1991**, *103*, 1419–1439; *Angew. Chem. Int. Ed. Engl.* **1991**, *30*, 1417–1436.

[23] X.-K. Jiang, G.-Z. Ji, B. Tu, X.-Y. Zhang, J.-L. Shi, X. Chen, *J. Am. Chem. Soc.* **1995**, *117*, 12679–12682.

[24] D. J. Abdallah, R.-G. Weiss, *Langmuir* **2000**, *16*, 351–355.

[25] S. Mann, *Angew. Chem.* **2000**, *112*, 3532–3548; *Angew. Chem. Int. Ed.* **2000**, *39*, 3392–3406.

[26] R. J. Bergeron, G. W. Yao, G. W. Erdos, S. Milstein, F. Gao, W. R. Weimar, O. Phanstiel, *J. Am. Chem. Soc.* **1995**, *117*, 6658–6665.

[27] M. Akazome, T. Takahashi, K. Ogura, *Tetrahedron Lett.* **1998**, *39*, 4839–4842.

[28] B. K. Vriesema, M. Lemaire, J. Buter, R. M. Kellogg, *J. Org. Chem.* **1986**, *51*, 5169–5177.

[29] L. Karle, D. Ranganathan, K. Shah and N. K. Vaishi, *Int. J. Peptide Protein Res.* **1994**, *43*, 160–165.

[30] A. G. Talma, P. Jouin, J. G. De Vries, C. B. Troostwijk, G. H. W. Buning, J. K. Waninge, J. Visscher, R. M. Kellogg, *J. Am. Chem. Soc.* **1985**, *107*, 3981–3997.

[31] A. L. Spek, *HELENA*, Program for Data Reduction, **1993**, University of Utrecht, Utrecht (The Netherlands).

[32] A. Altomare, M. C. Burla, M. Camalli, G. Cascarano, C. Giaccovazzo, A. Guagliardi, G. Polidori, *J. Appl. Crystallogr.* **1994**, *27*, 435–436.

[33] G. M. Sheldrick, *SHELX97*: Program for the Refinement of Crystal Structures, **1997**, Universität of Göttingen (Germany).

[34] A. L. Spek, PLATON98: *A Multipurpose Crystallographic Tool*, *120398 Version*, **1998**, University of Utrecht, Utrecht (The Netherlands).

[35] C. K. Johnson, ORTEPH, *Report ORNL-5138*, **1996**, Oak Ridge National Laboratory, Tennessee.

Received: July 24, 2000
Revised: February 26, 2001 [F2619]